

**Reply to Interactive comment on “Effect of Inorganic-to-Organic Mass Ratio on the Heterogeneous OH Reaction Rates of Erythritol: Implications for Atmospheric Chemical Stability of 2-Methyltetrols” by Rongshuang Xu et al.**

**5 Anonymous Referee #1**

Interactive comment on Atmos. Chem. Phys. Discuss., <https://doi.org/10.5194/acp-2019-981-RC1>, 2019

10 *This study examines the photochemical stability of pure erythritol particles and particles containing erythritol and ammonium sulfate (AS) against oxidation by OH radicals. Erythritol serves as a surrogate of 2-methyltetrols, a common compound of isoprene derived secondary organic aerosols. Reactive uptake of OH and subsequent degradation of erythritol in the particulate phase were determined as a function of inorganic-to-organic mass ratio (IOR). This was achieved using an aerosol flow reactor coupled to a soft atmospheric pressure ionization source (Direct Analysis in Real Time, DART) attached to a high-resolution mass spectrometer. It is found that the reactive uptake coefficient of OH decreases as the amount of AS increases. Furthermore, the results suggest that the reaction products due to OH oxidation are not significantly affected by the presence of AS. Since in the ambient methyltetrols are associated with AS, this study concludes that the chemical lifetime of methyltetrols is prolonged and may render methyltetrols stable against OH oxidation under humid conditions. The topic of this study fits well within the scope of ACP. I do not have major comments on this work, mostly minor ones and technical in nature. However, I suggest to carefully proofread the manuscript to improve the English language.*

15  
20

**We would like to sincerely thank the reviewer for his/her thoughtful comments. The referee's comments are below in italics followed by our responses.**

25

**Comment #1:**

*P. 9, top paragraph: Just a comment to better understand the origin of  $\text{HSO}_4^-$ . As the particles are heated and vaporize (ammonia is gone), the  $\text{SO}_4^{2-}$  can abstract a hydrogen from the organic molecule? This leads to the detection of  $\text{HSO}_4^-$ ? Since  $\text{HSO}_4^-$  signal does not change significantly between non-oxidized and the oxidized case, reactivity of OH with  $\text{SO}_4^{2-}$  or  $\text{HSO}_4^-$  (and maybe  $\text{NH}_4^+$ ) is not significant? A bit of rewording and better integration of previous studies would make this section easier to understand.*

30

**35 Author Response:**

Thanks for the comments. We would argue that sulfate ion ( $\text{SO}_4^{2-}$ ) is not an oxidant and cannot abstract a hydrogen atom from an organic molecule to form bisulfate ion ( $\text{HSO}_4^-$ ). As discussed in the manuscript and in the literature,  $\text{HSO}_4^-$  likely originates from ammonium sulfate (AS). In our

experiments, before introduced to the ionization region, erythritol–AS particles were fully vaporized under high temperature inside the particle heater and may thus thermally decompose into gas-phase ammonia (NH<sub>3</sub>) and sulfuric acid (H<sub>2</sub>SO<sub>4</sub>) (Drewnick et al., 2015), which can be detected as HSO<sub>4</sub><sup>−</sup> via direct ionization (Hajslova et al., 2011; Lam et al., 2019a, b; Kwong et al., 2018a, b).

George and Abbatt (2010) have revealed that dry (NH<sub>4</sub>)<sub>2</sub>SO<sub>4</sub> surface is highly unreactive toward gas-phase OH radicals. Furthermore, the surface reaction between dissolved SO<sub>4</sub><sup>2−</sup> and gas-phase OH radicals is not efficient (Cooper and Abbatt, 1996; Anastasio and Newberg, 2007). We have added this information in the revised manuscript.

Page 9, Line 12: “The HSO<sub>4</sub><sup>−</sup> likely originated from AS. Before introduced to the ionization region, erythritol–AS particles were fully vaporized under high temperature and may thus thermally decompose into gas-phase NH<sub>3</sub> and H<sub>2</sub>SO<sub>4</sub> (Drewnick et al., 2015), which can be detected as HSO<sub>4</sub><sup>−</sup> via direct ionization (Hajslova et al., 2011; Lam et al., 2019a, b; Kwong et al., 2018a, b). The intensity of HSO<sub>4</sub><sup>−</sup> before and after oxidation (Figure S1, *supplementary material*) showed no significant change, which is consistent with the argument in previous studies (Cooper and abbatt, 1996; Anastasio and Newberg, 2007) that the surface reaction between dissolved sulfate ions and gas-phase OH radicals is not efficient.”

**Comment #2:**

*Derivation of the OH uptake coefficient necessitates the particle diameter. It appears that a polydisperse aerosol was applied. It would be helpful to plot the aerosol size distribution or give the corresponding distribution parameters. Did the authors measure the aerosol distribution before and after oxidation to assess potential volatilization of the particles upon oxidation?*

**Author Response:**

Thanks for the comments. In our experiments, polydisperse particles were applied and the geometric standard deviation was 1.2–1.3. We acknowledge that the span of polydisperse particles could have effects on the determination of effective OH uptake coefficient,  $\gamma_{\text{eff}}$ . Further study which measures the  $\gamma_{\text{eff}}$  for both size-selected monodisperse and polydisperse particles is desired to better investigate the effect of particle size distribution on  $\gamma_{\text{eff}}$  calculation. As the spread of particle size in this work is small, we postulate that it would not significantly affect the determination of  $\gamma_{\text{eff}}$ .

We have observed slight changes in particle size upon oxidation for both erythritol and erythritol–AS particles (please see the **Figure S2** below). The surface-weighted mean diameter changes from 276.1 nm to 255.8 nm (~ 7.3 %) for erythritol particles and decreases from 278.2 nm to 262.1 nm (~ 5.8 %), from 280.5 nm to 266.7 nm (~ 4.9 %), from 281.2 nm to 274.0 nm (~ 2.6 %) for erythritol–AS particles at IOR = 0.5, 1.0 and 5.0, respectively. The decrease in particle size could be explained by the formation and volatilization of some reaction products proposed in the reaction scheme (i.e. C<sub>4</sub>

hydroxyketone and hydroxyaldehyde ( $C_4H_8O_4$ ),  $C_2$  hydroxyketone ( $C_2H_4O_2$ ) and  $C_3$  hydroxyaldehyde ( $C_3H_6O_3$ ).

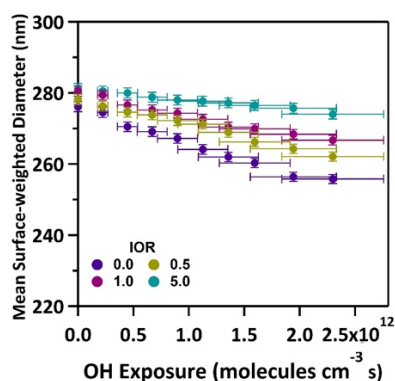


**Figure S2.** The change in surface-weighted mean diameter as a function of OH exposure for erythritol particles and erythritol-AS particles with different IORs.

*Supporting material*, we have added **Figure S2** in the *supporting material* to illustrate the change in particle diameter for erythritol particles and erythritol-AS particles upon oxidation.

Page 10, Line 21: “Further, the initial effective OH uptake coefficient,  $\gamma_{\text{eff}}$ , defined as the fraction of OH collisions with erythritol molecule that result in a reaction, can be computed (Kessler et al., 2010; Davies and Wilson, 2015),”

Page 11, Line 2: “For erythritol particles, the initial mean surface-weighted particle diameter was 276.1 nm and decreased to 255.8 nm after oxidation ( $\sim 7.3\%$ ).”

Page 11, Line 9: “For erythritol-AS particles, the particle diameters were measured to be 278.2–281.5 nm before oxidation (Table 1). Slight decreases in particle diameter ( $\sim 5.8\%$ ,  $\sim 4.9\%$ ,  $\sim 2.6\%$  at IOR = 0.5, 1.0 and 5.0, respectively) were also observed (*Figure S2, supplementary material*).”

Page 11, Line 19: “The  $\gamma_{\text{eff}}$  is found to decrease from  $0.45 \pm 0.025$  to  $0.02 \pm 0.001$  when the IOR increases from 0.0 to 5.0. We acknowledge that the span of polydisperse particles could have effects on the determination of  $\gamma_{\text{eff}}$ . Further study which measures the  $\gamma_{\text{eff}}$  for size selected monodisperse and polydisperse particles is desired to better investigate the effect of particle size distribution on  $\gamma_{\text{eff}}$  calculation.”

### Comment #3:

*How is the uncertainty of presented uptake values derived? Likely the width of the aerosol size distribution and the uncertainty in AIOMFC derived mfs values contribute to the overall uncertainty?*

### Author Response:

The uncertainty of effective OH uptake coefficient,  $\gamma_{\text{eff}}$  is calculated according to the error propagation rule:

$$\sigma_{\gamma} = \gamma_{\text{eff}} * \sqrt{\left(\frac{\sigma_k}{k}\right)^2 + \left(\frac{\sigma_{D0}}{D_0}\right)^2 + \left(\frac{\sigma_{\rho}}{\rho}\right)^2 + \left(\frac{\sigma_{mfs}}{mfs}\right)^2} \quad (\text{Eqn.1})$$

where  $\gamma_{\text{eff}}$  is the effective OH uptake coefficient,  $\sigma_{\gamma}$  is the uncertainty of effective OH uptake coefficient,  $k$  is the measured effective heterogeneous OH rate constant,  $\sigma_k$  is the uncertainty of effective heterogeneous OH rate constant,  $D_0$  is the mean surface-weighted diameter,  $\sigma_{D0}$  is the uncertainty of the mean surface-weighted particle diameter ( $\pm 0.5$  % uncertainty),  $mfs$  is the mass fraction of solute,  $\sigma_{mfs}$  is the uncertainty of mass fraction of solute ( $\pm 0.02$  for erythritol particles (Marsh et al., 2017),  $\pm 5$  %  $mfs$  for erythritol–AS particles predicted by AIOMFAC),  $\rho$  is the estimated particle density based on the volume additivity rule,  $\sigma_{\rho}$  is the uncertainty of particle density (determined based on following equation, Eqn.2)

$$\sigma_{\rho} = \rho^2 \frac{IOR * \rho_o * \rho_w + \rho_w * \rho_{AS} - (IOR + 1) * \rho_o * \rho_{AS}}{\rho_o * \rho_w * \rho_{AS}} * \sigma_{mfs} \quad (\text{Eqn.2})$$

where  $\rho_w$  is the water density ( $1.0 \text{ g cm}^{-3}$ ),  $\rho_o$  is the erythritol density ( $1.451 \text{ g cm}^{-3}$ ),  $\rho_{AS}$  is the density of AS ( $1.77 \text{ g cm}^{-3}$ ),  $IOR$  is the inorganic-to-organic ratio. From the calculations, the uncertainty in particle diameter has minor effect on  $\sigma_{\gamma}$  (less than 1 % at all IORs), while the uncertainty in  $mfs$  contributes about  $\sim 90$  % at all IORs when determining  $\sigma_{\gamma}$ .

#### Comment #4:

*Addition of the MD simulation is a neat feature. However, its validity depends strongly on established parameters, applied fields, etc. It would have been nice to show that the simulated system or another test case behaves as expected. Here, things may get more complicated since  $\text{NH}_4^+$  and  $\text{SO}_4^{2-}$  ions will be differently distributed within the particles? This could not be addressed as stated in text but could be discussed looking at previous studies (e.g., Tobias and Jungwirth groups).*

#### Author Response:

Thanks for the comment. While the previous studies such as that by Tobias and Jungwirth (2001) suggest that the propensity of a species for the air-water interface can depend strongly on the MD force fields used, our explanation is based on two general physical observations that do not depend strongly on the model parameters. Our first observation is that the probability for an impinging OH radical to collide near an erythritol molecule decreases as the concentration of erythritol decreases when there is more water due to the hygroscopicity of a salt. A lower concentration of erythritol leading to a smaller collision probability should not be model-specific. The second observation is that the average distance

between an OH radical and an erythritol molecule increases as their concentrations decrease because of more water. This again is a physical argument that does not depend strongly on the models used.

**Comment #5:**

- 5 *P. 12., l. 10-13: Please be more specific. Do you expect salting in or salting out for the particle systems you investigated? Will it change for the different IOR?*

**Author Response:**

10 To our best knowledge, the surface-bulk-partitioning behavior of erythritol when mixed with ammonium sulfate (AS) has not been experimentally measured. Ekström et al. (2009) have measured the surface tension using a FTÅ 125 tensiometer and have reported that when AS was added into 2-methylerythritol (with chemical structures similar to erythritol), the surface tension,  $\sigma$  was found to increase compared to that of 2-methylerythritol. For instance, for the system with 17 wt % of AS and 0.05 M of 2-methylerythritol, the surface tension was  $\sim 72.6 \text{ mN m}^{-1}$ , which is larger than that for 2-methylerythritol/water system ( $\sigma (0.05 \text{ M}) = \sim 69.7 \text{ mN m}^{-1}$ ). In their study, the surface tension increased from  $\sim 50.3 \text{ mN m}^{-1}$  to  $72.6 \text{ mN m}^{-1}$  when IOR increased from  $\sim 0.8$  to  $\sim 25.0$ , suggesting a salting in effect.

Composition	Surface tension ( $\text{mN m}^{-1}$ )	Molar concentration of 2-methylerythritol (M)
2-methylerythritol	$-14.3 \text{ c(M)} + 70.4$	0.02 – 1.87
2-methylerythritol + (17 % wt/wt) AS	$-15.1 \text{ c(M)} + 73.4$	0.05 – 1.53 <sup>a</sup>

20 <sup>a</sup> the range of molar concentration of erythritol in our work is from 0.59 M at IOR=5.0 to 4.5 M at IOR=0.0. And the corresponding IOR for 2-methylerythritol/AS/water mixture ranges from  $\sim 0.8$  to  $\sim 25.0$ .

25 On the other hand, Riva et al. (2019) have recently observed an interfacial tension depression using a biphasic microfluidic platform when AS is mixed with 2-methyltetrols (1.55 M of AS and 0.37 M of 2-methyltetrols (IOR =  $\sim 4.1$ )). This suggests a salting out effect. Based on these two results, the salt effect on the surface-bulk-partitioning behavior of 2-methyltetrols and likely erythritol remains unclear. Future investigations are needed to measure the surface tension for erythritol and erythritol – AS systems at different IORs in order to better understand the effect of salt on surface-bulk-partitioning behavior of erythritol within the particle and overall heterogeneous reactivity. We have added the following information in the revised manuscript.

Page 13, Line 4: “To our best knowledge, the surface-bulk-partitioning behavior of erythritol molecules in the presence of AS has not been experimentally measured. Ekström et al. (2009) have measured the

surface tension using a FTA 125 tensiometer and have reported that when AS was mixed with 2-methylerythritol (with chemical structures similar to erythritol), the surface tension,  $\sigma$  was found to increase compared to that of 2-methylerythritol. For instance, for the system with 17 wt % of AS and 0.05 M of 2-methylerythritol, the surface tension was  $\sim 72.6 \text{ mN m}^{-1}$ , which is larger than that for 2-methylerythritol/water system ( $\sigma (0.05 \text{ M}) = \sim 69.7 \text{ mN m}^{-1}$ ). In their study, the surface tension increased from  $\sim 50.3 \text{ mN m}^{-1}$  to  $72.6 \text{ mN m}^{-1}$  when IOR increased from  $\sim 0.8$  to  $\sim 25.0$ , suggesting a salting in effect. On the other hand, Riva et al. (2019) have recently observed an interfacial tension depression using a biphasic microfluidic platform when AS was mixed with 2-methyltetrols (1.55 M of AS and 0.37 M of 2-methyltetrols (IOR =  $\sim 4.1$ )), suggesting a salting out effect. Based on these two results, the salt effect on the surface-bulk-partitioning behavior of 2-methyltetrols and likely erythritol remains unclear. Future investigations which can well represent the distribution of erythritol molecules at the particle surface are desirable to better understand how the presence of salts would alter the surface concentration of organic molecule and ultimately affect its heterogeneous reactivity.”

**Comment #6:**

*Figure 2b: The legends using color bars are a bit confusing and maybe, I misunderstand those. Does the color coding of the experimental data has a relationship with the color coding of the ambient sulfate to 2-methyltetrol ratio? No ambient data is plotted and thus one wonders the meaning of that legend. The text already stated that the ambient ratio is much higher than the one probed in experiments. Same with the sulfate to erythritol ratio. There is no change in the color bar and the data are not plotted as a function of this ratio. This could be done by using a 3D plot. Also, the legends are not described in figure caption.*

**Author Response:**

We are sorry for the confusion. We have modified the Figure 2 in the revised manuscript. The color scale represents the range of sulfate to erythritol mass ratio (0 – 3.7) at different IORs in this work, much smaller than that for ambient mass ratio of sulfate to 2-methyltetrols reported in field studies ( $\sim 1.89 - \sim 250$ ). Legends are described in the figure caption in the revised manuscript.

Page 36, Line 1: “

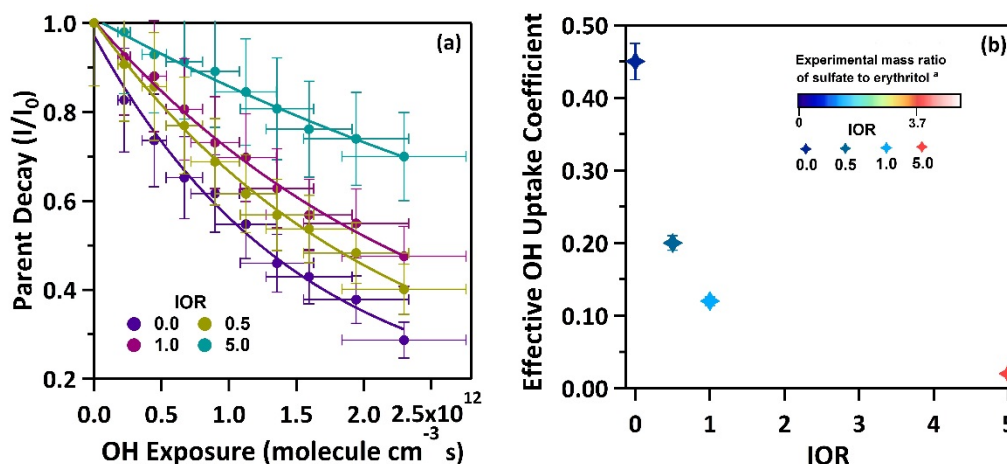


**Figure 2.** (a) The normalized decay of erythritol as a function of OH exposure during the heterogeneous OH oxidation of erythritol particles and erythritol-AS particles with different IORs. (b) The effective OH uptake coefficient,  $\gamma_{\text{eff}}$ . The data points represent  $\gamma_{\text{eff}}$  value at different IORs. The color scale represents the range of sulfate to erythritol mass ratio (0 – 3.7) at different IORs in this work, much smaller than that for ambient mass ratio of sulfate to 2-methyltetrols reported in field studies ( $\sim 1.89 - \sim 250$ ).’’

**Comment #7:**

*p. 1, l. 26: ...inorganic salts often coexist in atmospheric...*

**Author Response:**

We have changed this sentence in the revised manuscript.

Page 1, Line 25: “Additional uncertainty could raise since organic compounds and inorganic salts often coexist in atmospheric particles.”

**Comment #8:**

*p. 9, l. 1: The  $\text{HSO}_4^-$  likely originated...*

**Author Response:**

We have revised this sentence.

Page 9, Line 12: “The  $\text{HSO}_4^-$  likely originated from AS.”

**Comment #9:**

*p. 9, l. 5: ...before and after oxidation (...) showed no significant change...*

**Author Response:**

We have revised the sentence.

Page 9, Line 15: “The intensity of  $\text{HSO}_4^-$  before and after oxidation (Figure S1, *supplementary material*) showed no significant change,”

**References:**

- Anastasio, C. and Newberg, J. T.: Sources and sinks of hydroxyl radical in sea-salt particles, *J. Geophys. Res.: Atmos.*, 112, doi:10.1029/2006jd008061, 2007.
- Bethel, H. L., Atkinson, R. and Arey, J.: Hydroxycarbonyl products of the reactions of selected diols with the OH radical, *J. Phys. Chem. A*, 107, 6200–6205, doi:10.1021/jp027693l, 2003.
- Blanksby, S. J. and Ellison, G. B.: Bond Dissociation Energies of Organic Molecules, *ChemInform*, 34, doi:10.1002/chin.200324299, 2003.
- Block, E., Dane, A. J., Thomas, S., Cody, R. B.: Applications of Direct Analysis in Real Time Mass Spectrometry (DART-MS) in Allium Chemistry. 2-Propenesulfenic and 2-Propenesulfinic Acids, Diallyl Trisulfane S-Oxide, and Other Reactive Sulfur Compounds from Crushed Garlic and Other Alliums, *J. Agric. Food Chem.*, 58, 4617–4625, 2010.
- Cooper, P. L. and Abbatt, J. P. D.: Heterogeneous Interactions of OH and  $\text{HO}_2$  Radicals with Surfaces Characteristic of Atmospheric Particulate Matter, *J. Phys. Chem.*, 100, 2249–2254, doi:10.1021/jp952142z, 1996.
- Davies, J. F. and Wilson, K. R.: Nanoscale interfacial gradients formed by the reactive uptake of OH radicals onto viscous aerosol surfaces, *Chem. Sci.*, 6, 7020–7027, doi:10.1039/c5sc02326b, 2015.
- Drewnick, F., Diesch, J.-M., Faber, P. and Borrmann, S.: Aerosol mass spectrometry: particle–vaporizer interactions and their consequences for the measurements, *Atmos. Meas. Tech.*, 8, 3811–3830, doi:10.5194/amt-8-3811-2015, 2015.



- Ekström, S., Nozière, B., and Hansson, H.: The cloud condensation nuclei (CCN) properties of 2-methyltetrols and C<sub>3</sub>-C<sub>6</sub> polyols from osmolality and surface tension measurements. *Atmos. Chem. Phys.*, 9, 973–980. doi:10.5194/acp-9-973-2009, 2009.
- Hajslova, J., Cajka, T., and Vaclavik, L.: Challenging applications offered by direct analysis in real time (DART) in food-quality and safety analysis, *TrAC-Trend Anal. Chem.*, 30, 204–218, <https://doi.org/10.1016/j.trac.2010.11.001>, 2011.
- Kessler, S. H., Smith, J. D., Che, D. L., Worsnop, D. R., Wilson, K. R. and Kroll, J. H.: Chemical sinks of organic aerosol: kinetics and products of the heterogeneous oxidation of erythritol and levoglucosan, *Environ. Sci. Technol.*, 44, 7005–7010, doi:10.1021/es101465m, 2010.
- 10 Kwong, K. C., Chim, M. M., Hoffmann, E. H., Tilgner, A., Herrmann, H., Davies, J. F., Wilson, K. R. and Chan, M. N.: Chemical transformation of methanesulfonic acid and sodium methanesulfonate through heterogeneous OH oxidation, *ACS Earth Space Chem.*, 2, 895–903, doi:10.1021/acsearthspacechem.8b00072, 2018a.
- Kwong, K. C., Chim, M. M., Davies, J. F., Wilson, K. R. and Chan, M. N.: Importance of sulfate  
15 radical anion formation and chemistry in heterogeneous OH oxidation of sodium methyl sulfate, the smallest organosulfate, *Atmos. Chem. Phys.*, 18, 2809–2820, doi:10.5194/acp-18-2809-2018, 2018b.
- Lam, H. K., Shum, S. M., Davies, J. F., Song, M., Zuend, A., and Chan, M. N.: Effects of inorganic salts on the heterogeneous OH oxidation of organic compounds: insights from methylglutaric acid–ammonium sulfate, *Atmos. Chem. Phys.*, 19, 9581–9593, <https://doi.org/10.5194/acp-19-9581-2019>,  
20 2019a.
- Marsh, A., Miles, R. E. H., Rovelli, G., Cowling, A. G., Nandy, L., Dutcher, C. S. and Reid, J. P.: Influence of organic compound functionality on aerosol hygroscopicity: dicarboxylic acids, alkyl-substituents, sugars and amino acids, *Atmos. Chem. Phys.*, 17, 5583–5599, doi:10.5194/acp-17-5583-2017, 2017.
- 25 Riva, M., Chen, Y., Zhang, Y., Lei, Z., Olson, N. E., Boyer, H. C., Narayan, S., Yee, L. D., Green, H. S., Cui, T., Zhang, Z., Baumann, K., Fort, M., Edgerton, E., Budisulistiorini, S. H., Rose, C. A., Ribeiro,

- I. O., Oliveira, R. L. E., Santos, E. O. D., Machado, C. M. D., Szopa, S., Zhao, Y., Alves, E. G., Sá, S. S. D., Hu, W., Knipping, E. M., Shaw, S. L., Junior, S. D., Souza, R. A. F. D., Palm, B. B., Jimenez, J.-L., Glasius, M., Goldstein, A. H., Pye, H. O. T., Gold, A., Turpin, B. J., Vizuete, W., Martin, S. T., Thornton, J. A., Dutcher, C. S., Ault, A. P. and Surratt, J. D.: Increasing Isoprene Epoxydiol-to-Inorganic Sulfate Aerosol Ratio Results in Extensive Conversion of Inorganic Sulfate to Organosulfur Forms: Implications for Aerosol Physicochemical Properties, *Environ. Sci. Technol.*, 53, 8682–8694, doi:10.1021/acs.est.9b01019, 2019.
- Jungwirth, P. and Tobias, D. J.: Molecular Structure of Salt Solutions: A New View of the Interface with Implications for Heterogeneous Atmospheric Chemistry, *J. Phys. Chem. B*, 105, 10468–10472, doi:10.1021/jp012750g, 2001.

**Reply to Interactive comment on “Effect of Inorganic-to-Organic Mass Ratio on the Heterogeneous OH Reaction Rates of Erythritol: Implications for Atmospheric Chemical Stability of 2-Methyltetrols” by Rongshuang Xu et al.**

**5 Anonymous Referee #2**

Interactive comment on Atmos. Chem. Phys. Discuss., <https://doi.org/10.5194/acp-2019-981-RC2>, 2019

*Xu et al. investigated the OH-initiated heterogeneous oxidation of erythritol particles and particles containing erythritol and ammonium sulfate (AS). Erythritol was used as a surrogate of 2-methyltetrols, one of the most important isoprene-derived SOA products. SOA chemical composition was retrieved using a soft atmospheric pressure ionization source (DART) coupled to an Orbitrap. The reactivity of erythritol was characterized as a function of inorganic-to-organic mass ratio. While the study is well constrained and clearly presents some interesting results, some aspects are not considered within the discussion (see comments below).*

**We would like to sincerely thank the reviewer for his/her thoughtful comments. The referee's comments are below in italics followed by our responses.**

**20 Comment #1:**

*Page 2, lines 23-24: The authors stated that the reactivity of 2-methyltetrols has not been tested before. That's not fully correct. Hu et al. (Jimenez's group) investigated the aging of ambient isoprene-derived SOA and found that IEPOX-SOA (mainly producing 2-MT) are fairly unreactive. This study should be cited by the authors and further discuss.*

**Author Response:**

We would like to thank the reviewer for bringing up this paper by Hu et al. (2016). This work investigated the heterogenous reactivity of ambient IEPOX-SOA towards OH radical and reported reaction kinetics ( $4.0 \pm 2.0 \times 10^{-13} \text{ cm}^3 \text{ molecule}^{-1} \text{ s}^{-1}$  and  $3.9 \pm 1.8 \times 10^{-13} \text{ cm}^3 \text{ molecule}^{-1} \text{ s}^{-1}$  for IEPOX-SOA collected in SE US and Amazon, respectively) based on the decay of  $\text{C}_5\text{H}_6\text{O}^+$  ion (a tracer ion for IEPOX-SOA in ambient particles) in their AMS measurements. Based on these data, they calculated on average a more than 2-week ( $19 \pm 9$  days) atmospheric lifetime of IEPOX-SOA against OH radical oxidation based on rate constant of  $4.0 \pm 2.0 \times 10^{-13} \text{ cm}^3 \text{ molecule}^{-1} \text{ s}^{-1}$  and averaged ambient OH concentration of  $1.5 \times 10^6 \text{ molecule cm}^{-3}$ . We would like to acknowledge that these measured values are for ambient IEPOX-SOA and not for pure 2-methyltetrols. To our best knowledge, the heterogeneous OH reactivity of pure 2-methyltetrols particles has been investigated.

We agree with the reviewer that 2-methyltetrols are important components of IEPOX-SOA in the atmosphere. For instance, 2-methyltetrols can account for 10 % – 20 % of IEPOX-SOA in an experimental study (Surratt et al., 2010) and ~ 24 % of ambient IEPOX-SOA in field studies in rural Alabama, southeastern US (Isaacman et al., 2014). As suggested by Hu et al. (2016), the rates derived in their study could be considered as a lower limit for individual molecular components of IEPOX-SOA (e.g. 2-methyltetrols), as it may take two or more OH reactions for their AMS spectrum to no longer resemble that of IEPOX-SOA. We have added this information in the revised manuscript.

Page 3, Line 5: “Hu et al. (2016) have investigated the heterogeneous reactivity of ambient IEPOX-SOA (consisting of 2-methyltetrols, C5-alkene triols, organosulfate, etc.) towards gas-phase OH radicals in SE US and Amazon and reported the reaction kinetics for IEPOX-SOA based on the decay of C<sub>5</sub>H<sub>6</sub>O<sup>+</sup> ion (a tracer ion for IEPOX-SOA in ambient particles) in their AMS measurements. They calculated on average a more than 2-week (19 ± 9 days) atmospheric lifetime of IEPOX-SOA against heterogeneous OH oxidation based on rate constant of 4.0 ± 2.0 × 10<sup>-13</sup> cm<sup>3</sup> molecule<sup>-1</sup> s<sup>-1</sup> and averaged ambient OH concentration of 1.5 × 10<sup>6</sup> molecule cm<sup>-3</sup>. They also suggest that the observed rates may consider as a lower limit for individual molecular components of IEPOX-SOA (e.g. 2-methyltetrols) because it may take two or more OH reactions to make their AMS spectrum distinguishable from that of IEPOX-SOA after oxidation (Hu et al., 2016).”

#### **Comment #2:**

*Page 3, lines 3-5: The authors should be careful here and do not overstate the impact of OH reactivity. A chemical lifetime of 2 weeks cannot be really classified as a "significant" reaction/loss.*

#### **Author Response:**

We agree with the reviewer's comment. We have revised this sentence in the manuscript.

Page 3, Line 3: “Kessler et al. (2010) reported that heterogeneous oxidation of pure erythritol particles by gas-phase OH radicals with an effective OH uptake coefficient,  $\gamma_{\text{eff}}$ , of 0.77 ± 0.1 and a corresponding chemical lifetime of ~ 13.8 ± 1.4 days at a relative humidity (RH) of 30 %.”

#### **Comment #3:**

*Page 4, lines 26: The authors should provide more information regarding the experimental conditions: - What was the gas-phase concentration of erythritol? Is it possible that larger IOR lead to higher degassing (e.g., salting-out effect?) - Can the presence of gaseous erythritol decrease the concentration of OH radicals and further impact the heterogeneous reactivity? - Please provide the size, surface area and mass of particles for each condition.*

### Author Response:

Thanks for the comments. We have mentioned in the manuscript that control experiments had been carried out to investigate the volatilization of erythritol under our experimental conditions. The mass spectra were measured when erythritol particles and erythritol–AS particles were removed from the particle stream by filtration using a particle filter before entering the heater for DART analysis. No obvious peak was observed in mass spectra, suggesting that there is insignificant amount of erythritol present in the gas phase under our experimental conditions. We would also like to mention that the effective saturation vapor pressure,  $C^*$  of erythritol before oxidation for pure erythritol and erythritol–AS systems is estimated based on the framework by Zuend and Seinfeld (2012), using the saturation vapor pressure predicted by EVAPORATION (Compernelle et al., 2011) and the activity coefficient derived from AIOMFAC. The  $C^*$  of erythritol is estimated to be  $0.686 \mu\text{g m}^{-3}$ ,  $0.792 \mu\text{g m}^{-3}$ ,  $0.921 \mu\text{g m}^{-3}$ ,  $1.60 \mu\text{g m}^{-3}$  at IOR = 0.0, 0.5, 1.0, 5.0, respectively (**Table 1** in the revised manuscript) and  $\sim 99\%$  of erythritol would be expected to remain in particle phase in all experiments based on gas-particle partitioning model (Zuend and Seinfeld, 2012) with the particle mass loading of about  $500 \mu\text{g m}^{-3}$  in our experiments. These results suggest that the volatilization and gas-phase reactivity of erythritol would not be significant in our work. We also acknowledge that the effects of the salt on the gas-particle partitioning of erythritol (in term of  $C^*$ ) have been considered by calculating the activity coefficients of erythritols using AIOMFAC at different IORs.

The surface-weighted mean diameter of erythritol and erythritol – AS particles at all IORs have been given in **Table 1**. The mass loading under all experiments was around  $500 \mu\text{g m}^{-3}$ , and the surface area was  $\sim 9 \times 10^9 \text{ nm}^2 \text{ cm}^{-3}$ .

### Comment #4:

*Page 6, dart section: Please provide more information. Was it real-time evaporation or were the particles collected onto a filter prior vaporization?*

### Author Response:

Thanks for the comment. In our experiments, it was a real-time evaporation of the particles. The particle stream was directed into a stainless-steel tube, where the particles were fully vaporized in real time. The resultant gas-phase species were then delivered into an ionization region. The erythritol particles and erythritol–AS particles were confirmed to be fully vaporized at  $300^\circ\text{C}$  before introduced to the ionization region in separate experiments, thus yielding a mass spectrum representative of the entire particle (i.e., bulk composition). We have added this information in the manuscript.

Page 5, Line 22: “The remaining flow was directed to a stainless-steel tube heater, where the particles were fully vaporized in real time. The resultant gas-phase species were then delivered into an ionization

region. The erythritol particles and erythritol–AS particles were confirmed to be fully vaporized at 300 °C before introduced to the ionization region in separate experiments, thus yielding a mass spectrum representative of the entire particle (i.e., bulk composition).”

5 **Comment #5:**

Page 9: *Recent studies have shown that isoprene-derived SOA, especially when formed in the presence of acidic aerosols are highly viscous, further impacting heterogeneous processes (e.e., Surratt’s group, Ault’s group, Thornton’s group). While the assumption that erythritol is well mixed is likely correct, the authors cannot ignore these recent studies and the last paragraph (i.e., atmospheric implications)*  
10 *should mention the impact of the phase and viscosity on the heterogeneous reactivity of isoprene derived SOA products. In other words, the rate constant/lifetimes proposed in this study are likely an upper limit suggesting that the OH oxidation of 2-methyltetrols is negligible.*

**Author Response:**

15 We agree with the reviewer’s comment that the particle phase, morphology and viscosity can significantly affect the heterogeneous reactivity of isoprene derived SOA and their individual components (e.g. 2-methyltetrols). When the isoprene derived SOA are highly viscous, this slows down the overall rate of reaction due to diffusion. In this study, the rate constants and lifetimes measured for well mixed erythritol particles and erythritol–AS particles at a high RH may consider as  
20 an upper limit. The OH oxidation of 2-methyltetrols in ambient particles could be slower than our reported values, depending on the formation pathways and composition of isoprene derived SOA and atmospheric conditions. We have added the following information in the conclusions.

Page 18, Line 22: “Recent studies have shown that the phase state and viscosity of the particles  
25 depending on the particle composition and environmental factors can significantly affect the diffusivity of organic molecules, water molecules and oxidants such as gas-phase OH radicals, which in turn the overall oxidation rate and formation of products (Chan et al., 2014; Slade and Knopf, 2014; Chim et al., 2017a; Marshall et al., 2016; 2018). Isoprene-derived SOA, especially when formed in the presence of acidic sulfate particles have been reported to be highly viscous (Shrivastava et al., 2017; Olson et al., 2019; Zhang et al., 2019). For instance, Riva et al. (2019) have shown that a viscous IEPOX-SOA  
30 coating was likely formed in the presence of acidic sulfate seed particles. The diffusion of organic molecules (e.g. 2-methyltetrols) from the bulk to the particle surface could slow down, lowering the overall heterogeneous reactivity.

35 To date, the effects of the complex interplay between particle phase, morphology and viscosity on the heterogeneous reactivity remains largely unexplored. We would like to acknowledge that in this study the rate constants and lifetimes measured for well mixed erythritol particles and erythritol–AS particles at a high RH may consider as an upper limit. The OH oxidation of 2-methyltetrols in ambient particles

could be slower than our reported values, depending on the formation pathways and composition of IEPOX-SOA and atmospheric conditions (e.g. RH and temperature). All these results suggest that a single kinetic parameter may not be well described for the heterogeneous OH oxidation erythritols and 2-methyltetrols in atmosphere since the rates can vary significantly, depending on the particle composition, phase and morphology and environmental factors.”

#### Comment #6:

Page 9, lines 11-14: Did the particles shrink? Did the authors estimate a carbon closure?

#### Author Response:

As discussed in our response for **reviewer 1**, **comment #7**, we have observed slight changes in particle size upon oxidation for both erythritol and erythritol-AS particles (please see the **figure** below). The surface-weighted mean diameter changes from 276.1 nm to 255.8 nm (~ 7.3 %) for erythritol particles and decreases from 278.2 nm to 262.1 nm (~ 5.8 %), from 280.5 nm to 266.7 nm (~ 4.9 %), from 281.2 nm to 274.0 nm (~ 2.6 %) for erythritol-AS particles at IOR = 0.5, 1.0 and 5.0, respectively. The decrease in particle size could be explained by the formation and volatilization of some reaction products (i.e. C<sub>4</sub> hydroxyketone and hydroxyaldehyde (C<sub>4</sub>H<sub>8</sub>O<sub>4</sub>), C<sub>2</sub> hydroxyketone (C<sub>2</sub>H<sub>4</sub>O<sub>2</sub>) and C<sub>3</sub> hydroxyaldehyde (C<sub>3</sub>H<sub>6</sub>O<sub>3</sub>)). We have added this information in the revised manuscript.

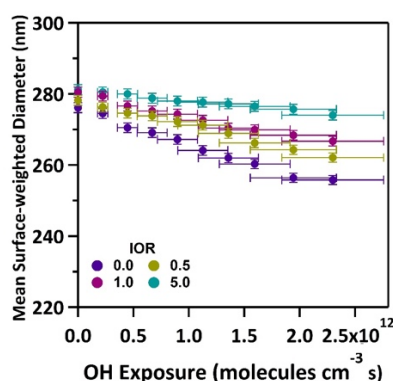


**Figure S2.** The change in surface-weighted mean diameter as a function of OH exposure for erythritol particles and erythritol-AS particles with different IORs.

*Supporting material*, we have added **Figure S2** in the *supporting material* to illustrate the change in particle diameter for erythritol particles and erythritol-AS particles upon oxidation.

Determining a carbon closure is a very good suggestion. However, we cannot estimate a carbon closure with a few reasons. One reason is that we may not be able to detect all reaction products with the DART-MS technique. Second, we cannot quantify the concentration of particle-phase products because the ionization efficiencies of the products are not known. At last, gas-phase products have not been

measured in our experiments. However, we agree with the reviewer a carbon closure study should be considered and carried out in future study.

**Comment #7:**

- 5 *Page 10, lines 9-10: That doesn't mean that thermal decomposition is not occurring for other types of compounds, e.g., carboxylic acid or other oxygenated species. As the authors did not report any concentrations it is not difficult to make such a statement; i.e., the observed compounds can be only a fraction of the quantity formed. In addition, the measured compounds can fragment into small ions:  $< m/z$  70. It is also unclear*
- 10 *why the authors selected such a narrow mass range. To fully investigate the potential fragmentation the authors could have extended the mass range: i.e., 50-400. Please clarify.*

**Author Response:**

- 15 Thanks for the comments. DART ion source is considered as a less energetic “soft” ionization technique, which applies less excess internal energy to the target molecule, resulting in minimal dissociation and yielding intact ions with minimal fragmentation. Previous studies (Cody et al., 2005; Nah et al., 2013) have shown that the dominant ions for their investigated organic compounds (M), including alkanes, alkenes, carboxylic acids, esters, and alcohols, in negative-ion mass spectra are
- 20 observed in the form of  $[M-H]^-$ , or  $[M]^-$ . These results suggest that the thermal decomposition of these classes of organic compounds may not be significant. However, we agree with the reviewer that some potential reaction products (e.g. oligomers and peroxides) could be thermally decomposed in our experiments.
- 25 We agree with the reviewer about the concerns about the thermal decomposition and quantification of the reaction products in our particle-DART technique. Since the ionization efficiency of erythritol and its reaction products are currently not well understood, we thus do not attempt to quantify their concentrations.
- 30 We chose this detected range because this gave the best overall performance when we optimized our systems. Thus, small ions which were less  $m/z$  70 were not measured in our work. In this work, we primarily focus on the measurement of reaction products remained in the particle phase after oxidation. However, we agree with the reviewer that it would be important to measure these small ions, which are likely volatile fragmentation products present in the gas phase. The measurement of gas-phase
- 35 products, together with the characterization of particle-phase products would provide better insight into heterogeneous reaction pathways.



**Comment #8:**

*Page 10, lines 13-14: Here again the statement is not correct. The authors have to be quantitative in order to make such a statement. For example, did the authors try to generate SOA with one single compound (e.g., carboxylic, polyol,...) and determine if*

5 *the mass measured with the DART corresponds to the mass measure with an SMPS?*

**Author Response:**

On page 10, Line 21, we calculated the effective OH uptake coefficient for erythritol particles and erythritol-AS particles. We have not tried to generate SOA for the OH oxidation in this work.

10

As raised by the reviewer in his/her earlier comment, we do not attempt to quantify the particle mass measured with the DART and compare the results with that measured with an SMPS. One reason is that the ionization efficiencies of the reaction products are not known and not all reaction products were detected by the DART. While we cannot quantify the concentration of the reaction products, we can quantify the OH decay of the erythritol upon oxidation using their normalized signal before and after oxidation (Eqn.4 in the manuscript). This method does not require to know the mass concentration of the species.

15

**Comment #9:**

*Page 10, line 17: What would be the expected fragment ions? Not all ions were identified in Fig 1 and some fragments ions were not present before the reaction. Please clarify.*

20

**Author Response:**

Thanks for the comments. In terms of the expected fragment ion, we could not find the statement on Page 10, line 17 in the original manuscript. We think the reviewer may refer to Page 9, line 20: “but there was no indication of fragment ions expected from...”. As mentioned in our response for **comment #7**, in the literature, the thermal decomposition of alcohols and carboxylic acids has not been observed and reported using particle-DART technique (Nah et al., 2013). However, we acknowledge that at high temperature organic peroxides may break down with the cleavage of O-O bond, and oligomers may also thermally decompose during the analysis to yield smaller fragmentation products (Mukundan and Kishore, 1990). The fragment ions could be difficult to identify depending on their chemical structures. Further investigation on the formation of these products during heterogeneous OH oxidation of organic compounds is desirable. We have revised our statement in the manuscript.

25

30

35

Page 10, Line 2: “However, we would like to note that some possible reaction products (e.g. organic peroxides and oligomers) could be formed from reactions between peroxy radicals (Stark et al., 2017). We do not rule out the formation of these products upon OH oxidation of erythritol as they may undergo

thermal decomposition at high temperature with the cleavage of O-O bond (Mukundan and Kishore, 1990). Further investigation on the formation of organic peroxides and oligomers upon heterogeneous OH oxidation of organic compounds is desirable.”

5 We do not attempt to identify all ions in particle-DART mass spectra. One reason is that these ions were minor peaks with their relative abundances less than 2% (We could not rule out that their concentrations could be high since their chemical identities and ionization efficiencies are not known). Details about these ions are summarized in following table. We would like to acknowledge that  $C_3H_3O_4^-$  ion ( $m/z = 103$ ) was detected after oxidation at IOR = 0.0 but have been observed before  
10 oxidation at other IORs. Similarly, for  $C_4H_3O_4^-$  ions ( $m/z = 115$ ), it has been detected before oxidation at IOR = 1.0 and 5.0. We would also like to note that a minor ion at  $m/z = 133$  ( $C_4H_5O_4^-$ ) was only presented after oxidation. Based on the suggested chemical formula, it may be a second-generation reaction product. To avoid confusion and overstatement, these three minor peaks were not discussed in this work.

15

$m/z$	Chemical formula	Relative abundance
New ion after oxidation at IOR = 0.0		
103	$C_3H_3O_4^-$	1.97 %
115	$C_4H_3O_4^-$	1.87 %
133	$C_4H_5O_5^-$	1.68 %
New ion after oxidation at IOR = 0.5		
115	$C_4H_3O_4^-$	1.86 %
133	$C_4H_5O_5^-$	1.33 %
New ion after oxidation at IOR = 1.0		
133	$C_4H_5O_5^-$	1.01 %
New ion after oxidation at IOR = 5.0		
133	$C_4H_5O_5^-$	0.51 %

#### Comment #10:

Page 10, Fig 2: Please explain the meaning of the error bars. Is it from different experiments?

20

#### Author Response:

In Figure 2. (a), the x-error bar represents the calculated error in the OH exposure. The OH exposure, defined as the products of gas-phase OH concentration, [OH], and the particle residence time,  $t$ , was determined by measuring the decay of the hexane (Smith et al., 2009):

25

$$OH \text{ exposure} = -\frac{\ln([Hex]/[Hex]_0)}{k_{Hex}} = \int_0^t [OH] dt \text{ (Eqn.1)}$$

where  $[Hex]$  is the hexane concentration leaving the reactor after oxidation,  $[Hex]_0$  is the initial hexane concentration before oxidation, and  $k_{Hex}$  is the second-order rate constant of the gas-phase OH–hexane reaction).

- 5 Based on Eqn.1 and the error propagation rule, the uncertainty for OH exposure,  $\sigma_{OH\ exp}$ , was derived from Eqn.2:

$$\sigma_{exp} = 0.005 (OH\ exposure) \sqrt{\left(16 + \frac{2}{(OH\ exposure \times k_{Hex})^2}\right)} \quad (\text{Eqn.2})$$

- where 0.005 is the precision of Hex measurement (0.5 % of the reading). The y-error is the error in  
 10 parent decay index ( $\frac{I}{I_0}$ ), where  $I$  is the signal intensity of erythritol at a given OH exposure,  $I_0$  is the signal intensity before oxidation. The y-error was determined from the following equation when the uncertainty of signal intensity was assigned to be 0.1 %:

$$\sigma_{\frac{I}{I_0}} = \frac{I}{I_0} \times 0.1 \times \sqrt{2} \quad (\text{Eqn.3})$$

In Figure 2. (b), the y-error represents the uncertainty of derived effective OH uptake coefficient.

15

#### **Comment #11:**

*Page 17, line 15: Is it possible to estimate any branching ratio? Is the DART technique more sensitive/selective for certain types of compounds?*

#### **Author Response:**

Thanks for the suggestion. Since the ionization efficiencies of erythritol and reaction products are not known, the relative abundance of the products after oxidation cannot be well quantified. Furthermore, we are not able to detect all reaction products in both gas- and particle-phases. We thus do not attempt to estimate the branching ratios.

25

We agree with the reviewer that it is important to know whether the DART technique is more sensitive/selective for certain types of compounds. In the literature, the sensitivity and detection limits for some organic compounds has been reported to be dependent on the structure and functionality of investigated compounds (Cody et al., 2005; Nah et al., 2013; Chan et al., 2014; Chim et al., 2017a).

- 30 For instance, Chan et al. (2014) have measured the ionization efficiency of oxalic acid, malonic acid, oxosuccinic acid, and tartaric acid relative to succinic acid and found these values can vary from 0.5 to 4.59 due to the change in carbon number ( $C_2$  to  $C_4$ ) and functional group (alcohol or ketone). To date, there are only limited classes of organic compounds were investigated. It remains largely unclear whether the particle-DART technique is more sensitive/selective for certain types of compounds. We  
 35 would also like to note that the experimental configuration (Chan et al., 2013) and other factors (e.g.

types of mass spectrometers) may have significant effects on the responses of organic compounds in the mass spectra (Nah et al., 2013). Cautions should be taken when we compare the results among different studies with various experimental configurations and conditions.

5 **Comment #12:**

page 5, line 5. Should molecule  $\text{cm}^{-3} \text{ s}$  be molecule  $\text{cm}^{-3} \text{ s}^{-1}$

**Author Response:**

10 The reviewer may refer to the unit of OH exposure. The OH exposure, defined as the products of gas-phase OH concentration,  $[\text{OH}]$ , and the particle residence time,  $t$ , was determined by measuring the decay of the hexane (Smith et al., 2009):

$$\text{OH exposure} = -\frac{\ln([\text{Hex}]/[\text{Hex}]_0)}{k_{\text{Hex}}} = \int_0^t [\text{OH}] dt \quad (\text{Eqn.1})$$

15 where  $[\text{Hex}]$  is the hexane concentration leaving the reactor after oxidation,  $[\text{Hex}]_0$  is the initial hexane concentration before oxidation, and  $k_{\text{Hex}}$  is the second-order rate constant of the gas-phase OH–hexane reaction ( $5.2 \times 10^{-12} \text{ cm}^3 \text{ molecule}^{-1} \text{ s}^{-1}$ ). Hence, the unit would be molecule  $\text{cm}^{-3} \text{ s}$ .

**Comment #13:**

page 6, line 7. It should be Orbitrap

20

**Author Response:**

We have revised the sentence.

25 Page 6, Line 1: “The gas-phase species leaving the heater were introduced into an atmospheric pressure ionization region, a narrow open space between the DART ionization source (IonSense: DART SVP), and the inlet orifice of the high-resolution mass spectrometer (Thermo Fisher, Q Exactive Orbitrap) for ionization and detection (Nah et al., 2013; Chan et al., 2013; 2014).”

30 **Reference:**

Chan, M. N., Zhang, H., Goldstein, A. H. and Wilson, K. R.: Role of water and phase in the heterogeneous oxidation of solid and aqueous succinic acid aerosol by hydroxyl radicals, J. Phys. Chem. C, 118, 28978–28992, doi:10.1021/jp5012022, 2014.

- Cheng, C. T., Chan, M. N. and Wilson, K. R.: Importance of unimolecular HO<sub>2</sub> elimination in the heterogeneous OH reaction of highly oxygenated tartaric acid aerosol, *J. Phys. Chem. A*, 120, 5887–5896, doi:10.1021/acs.jpca.6b05289, 2016.
- Chim, M. M., Chow, C. Y., Davies, J. F. and Chan, M. N.: Effects of relative humidity and particle  
5 phase water on the heterogeneous OH oxidation of 2-methylglutaric acid aqueous droplets, *J. Phys. Chem. A*, 121, 1666–1674, doi:10.1021/acs.jpca.6b11606, 2017a.
- Cody, R. B., Laramée, J. A. and Durst, H. D.: Versatile new ion source for the analysis of materials in open air under ambient conditions, *Anal. Chem.*, 77, 2297–2302, doi:10.1021/ac050162j, 2005.
- Compernelle, S., Ceulemans, K. and Müller, J.-F.: EVAPORATION: a new vapour pressure estimation  
10 method for organic molecules including non-additivity and intramolecular interactions, *Atmos. Chem. Phys.*, 11, 9431–9450, doi:10.5194/acp-11-9431-2011, 2011.
- Hu, W., Palm, B. B., Day, D. A., Campuzano-Jost, P., Krechmer, J. E., Peng, Z., Sá, S. S. D., Martin, S. T., Alexander, M. L., Baumann, K., Hacker, L., Kiendler-Scharr, A., Koss, A. R., Gouw, J. A. D., Goldstein, A. H., Seco, R., Sjostedt, S. J., Park, J.-H., Guenther, A. B., Kim, S., Canonaco, F., Prévôt,  
15 A. S. H., Brune, W. H. and Jimenez, J. L.: Volatility and lifetime against OH heterogeneous reaction of ambient isoprene-epoxydiols-derived secondary organic aerosol (IEPOX-SOA), *Atmos. Chem. Phys.*, 16, 11563–11580, doi:10.5194/acp-16-11563-2016, 2016.
- Isaacman, G., Kreisberg, N. M., Yee, L. D., Worton, D. R., Chan, A. W. H., Moss, J. A., Hering, S. V. and Goldstein, A. H.: Online derivatization for hourly measurements of gas- and particle-phase semi-  
20 volatile oxygenated organic compounds by thermal desorption aerosol gas chromatography (SV-TAG), *Atmos. Meas. Tech.*, 7, 4417–4429, doi:10.5194/amt-7-4417-2014, 2014.
- Kwong, K. C., Chim, M. M., Hoffmann, E. H., Tilgner, A., Herrmann, H., Davies, J. F., Wilson, K. R. and Chan, M. N.: Chemical transformation of methanesulfonic acid and sodium methanesulfonate through heterogeneous OH oxidation, *ACS Earth Space Chem.*, 2, 895–903,  
25 doi:10.1021/acsearthspacechem.8b00072, 2018a.

- Kwong, K. C., Chim, M. M., Davies, J. F., Wilson, K. R. and Chan, M. N.: Importance of sulfate radical anion formation and chemistry in heterogeneous OH oxidation of sodium methyl sulfate, the smallest organosulfate, *Atmos. Chem. Phys.*, 18, 2809–2820, doi:10.5194/acp-18-2809-2018, 2018b.
- Lam, H. K., Shum, S. M., Davies, J. F., Song, M., Zuend, A., and Chan, M. N.: Effects of inorganic salts on the heterogeneous OH oxidation of organic compounds: insights from methylglutaric acid–ammonium sulfate, *Atmos. Chem. Phys.*, 19, 9581–9593, <https://doi.org/10.5194/acp-19-9581-2019>, 2019a.
- Lam, H. K., Kwong, K. C., Poon, H. Y., Davies, J. F., Zhang, Z., Gold, A., Surratt, J. D. and Chan, M. N.: Heterogeneous OH oxidation of isoprene-epoxydiol-derived organosulfates: kinetics, chemistry and formation of inorganic sulfate, *Atmos. Chem. Phys.*, 19, 2433–2440, doi:10.5194/acp-19-2433-2019, 2019b.
- Marshall, F. H., Miles, R. E. H., Song, Y.-C., Ohm, P. B., Power, R. M., Reid, J. P. and Dutcher, C. S.: Diffusion and reactivity in ultraviscous aerosol and the correlation with particle viscosity, *Chem. Sci.*, 7, 1298–1308, doi:10.1039/c5sc03223g, 2016.
- Marshall, F. H., Berkemeier, T., Shiraiwa, M., Nandy, L., Ohm, P. B., Dutcher, C. S. and Reid, J. P.: Influence of particle viscosity on mass transfer and heterogeneous ozonolysis kinetics in aqueous-sucrose-maleic acid aerosol, *Phys. Chem. Chem. Phys.*, 20, 15560–15573, doi:10.1039/c8cp01666f, 2018.
- Mukundan, T. and Kishore, K.: Synthesis, characterization and reactivity of polymeric peroxides, *Prog. Poly. Sci.*, 15, 475–505, doi:10.1016/0079-6700(90)90004-k, 1990.
- Nah, T., Chan, M., Leone, S. R. and Wilson, K. R.: Real time in situ chemical characterization of submicrometer organic particles using direct analysis in Real Time-Mass Spectrometry, *Anal. Chem.*, 85, 2087–2095, doi:10.1021/ac302560c, 2013.
- Olson, N. E., Lei, Z., Craig, R. L., Zhang, Y., Chen, Y., Lambe, A. T., Zhang, Z., Gold, A., Surratt, J. D. and Ault, A. P.: Reactive Uptake of Isoprene Epoxydiols Increases the Viscosity of the Core of

- Phase-Separated Aerosol Particles, *ACS Earth Space Chem.*, **3**, 1402–1414, doi:10.1021/acsearthspacechem.9b00138, 2019.
- Riva, M., Chen, Y., Zhang, Y., Lei, Z., Olson, N. E., Boyer, H. C., Narayan, S., Yee, L. D., Green, H. S., Cui, T., Zhang, Z., Baumann, K., Fort, M., Edgerton, E., Budisulistiorini, S. H., Rose, C. A., Ribeiro, I. O., Oliveira, R. L. E., Santos, E. O. D., Machado, C. M. D., Szopa, S., Zhao, Y., Alves, E. G., Sá, S. S. D., Hu, W., Knipping, E. M., Shaw, S. L., Junior, S. D., Souza, R. A. F. D., Palm, B. B., Jimenez, J.-L., Glasius, M., Goldstein, A. H., Pye, H. O. T., Gold, A., Turpin, B. J., Vizuete, W., Martin, S. T., Thornton, J. A., Dutcher, C. S., Ault, A. P. and Surratt, J. D.: Increasing Isoprene Epoxydiol-to-Inorganic Sulfate Aerosol Ratio Results in Extensive Conversion of Inorganic Sulfate to Organosulfur Forms: Implications for Aerosol Physicochemical Properties, *Environ. Sci. Technol.*, **53**, 8682–8694, doi:10.1021/acs.est.9b01019, 2019.
- Shrivastava, M., Cappa, C. D., Fan, J., Goldstein, A. H., Guenther, A. B., Jimenez, J. L., Kuang, C., Laskin, A., Martin, S. T., Ng, N. L., Petaja, T., Pierce, J. R., Rasch, P. J., Roldin, P., Seinfeld, J. H., Shilling, J., Smith, J. N., Thornton, J. A., Volkamer, R., Wang, J., Worsnop, D. R., Zaveri, R. A., Zelenyuk, A. and Zhang, Q.: Recent advances in understanding secondary organic aerosol: Implications for global climate forcing, *Rev. Geophys.*, **55**, 509–559, doi:10.1002/2016rg000540, 2017.
- Smith, J. D., Kroll, J. H., Cappa, C. D., Che, D. L., Liu, C. L., Ahmed, M., Leone, S. R., Worsnop, D. R. and Wilson, K. R.: The heterogeneous reaction of hydroxyl radicals with sub-micron squalane particles: a model system for understanding the oxidative aging of ambient aerosols, *Atmos. Chem. Phys.*, **9**, 3209–3222, doi:10.5194/acp-9-3209-2009, 2009.
- Stark, H., Yatavelli, R. L. N., Thompson, S. L., Kang, H., Krechmer, J. E., Kimmel, J. R., Palm, B. B., Hu, W. W., Hayes, P. L., Day, D. A., Campuzano-Jost, P., Canagaratna, M. R., Jayne, J. T., Worsnop, D. R., and Jimenez, J. L.: Impact of Thermal Decomposition on Thermal Desorption Instruments: Advantage of Thermogram Analysis for Quantifying Volatility Distributions of Organic Species, *Environ. Sci. Technol.*, **51**, 8491–8500, 2017.

- Surratt, J. D., Chan, A. W. H., Eddingsaas, N. C., Chan, M., Loza, C. L., Kwan, A. J., Hersey, S. P., Flagan, R. C., Wennberg, P. O. and Seinfeld, J. H.: Reactive intermediates revealed in secondary organic aerosol formation from isoprene, *Proc. National Acad. Sci.*, 107, 6640–6645, doi:10.1073/pnas.0911114107, 2010.
- 5 Zhang, Y., Chen, Y., Lei, Z., Olson, N. E., Riva, M., Koss, A. R., Zhang, Z., Gold, A., Jayne, J. T., Worsnop, D. R., Onasch, T. B., Kroll, J. H., Turpin, B. J., Ault, A. P. and Surratt, J. D.: Joint Impacts of Acidity and Viscosity on the Formation of Secondary Organic Aerosol from Isoprene Epoxydiols (IEPOX) in Phase Separated Particles, *ACS Earth Space Chem.*, 3, 2646–2658, doi:10.1021/acsearthspacechem.9b00209, 2019.
- 10 Zhou, S., Forbes, M. W. and Abbatt, J. P. D.: Application of Direct Analysis in Real Time-Mass Spectrometry (DART-MS) to the Study of Gas–Surface Heterogeneous Reactions: Focus on Ozone and PAHs, *Anal. Chem.*, 87, 4733–4740, doi:10.1021/ac504722z, 2015.
- Zuend, A. and Seinfeld, J. H.: Modeling the gas-particle partitioning of secondary organic aerosol: the importance of liquid-liquid phase separation, *Atmos. Chem. Phys.*, 12, 3857–3882, doi:10.5194/acp-12-3857-2012, 2012.
- 15



# Effect of Inorganic-to-Organic Mass Ratio on the Heterogeneous OH Reaction Rates of Erythritol: Implications for Atmospheric Chemical Stability of 2-Methyltetrols

5 Rongshuang Xu<sup>1</sup>, Hoi Ki Lam<sup>1</sup>, Kevin R. Wilson<sup>2</sup>, James F. Davies<sup>3</sup>, Mijung Song<sup>4</sup>, Wentao Li<sup>5</sup>, Ying-Lung Steve Tse<sup>5</sup>, Man Nin Chan <sup>1,6</sup>

<sup>1</sup>Earth System Science Programme, Faculty of Science, The Chinese University of Hong Kong, Hong Kong, China

10 <sup>2</sup>Chemical Sciences Division, Lawrence Berkeley National Laboratory, Berkeley, CA, USA

<sup>3</sup>Department of Chemistry, University of California Riverside, Riverside, CA, USA

<sup>4</sup>Department of Earth and Environmental Sciences, Jeonbuk National University, Jeollabuk-do, Republic of Korea

<sup>5</sup>Department of Chemistry, The Chinese University of Hong Kong, Hong Kong, China

15 <sup>6</sup>The Institute of Environment, Energy and Sustainability, The Chinese University of Hong Kong, Hong Kong, China

Corresponding author: mnchan@cuhk.edu.hk

## 20 Abstract

2-methyltetrols have been widely chosen as chemical tracers for isoprene-derived secondary organic aerosols. While they are often assumed to be relatively unreactive, a laboratory study reported that pure erythritol particles (an analog of 2-methyltetrols) can be heterogeneously oxidized by gas-phase OH radicals at a significant rate. This might question the efficacy of these compounds as tracers in aerosol source apportionment studies. Additional uncertainty could arise since organic compounds and inorganic salts are often coexisting in atmospheric particles. To gain more insights into the chemical

25

stability of 2-methyltetrols in atmospheric particles, this study investigates the heterogeneous OH oxidation of pure erythritol particles and particles containing erythritol and ammonium sulfate (AS) at different dry inorganic-to-organic mass ratios (IOR) in an aerosol flow tube reactor at a high relative humidity of 85 %. The same reaction products are formed upon heterogeneous OH oxidation of erythritol and erythritol-AS particles, suggesting that the reaction pathways are not strongly affected by the presence and amount of AS. On the other hand, the effective OH uptake coefficient,  $\gamma_{\text{eff}}$ , is found to decrease by about a factor of  $\sim 20$  from  $0.45 \pm 0.025$  to  $0.02 \pm 0.001$  when the relative abundance of AS increases and the IOR increases from 0.0 to 5.0. One likely explanation is the presence of dissolved ions slows down the reaction rates by decreasing the surface concentration of erythritol and reducing the frequency of collision between erythritol and gas-phase OH radicals at the particle surface. Hence, the heterogeneous OH reactivity of erythritol and likely 2-methyltetrols in atmospheric particles would be slower than previously thought when the salts are present. Given 2-methyltetrols often coexist with a significant amount of AS in many environments, where ambient IOR can vary from  $\sim 1.89$  to  $\sim 250$ , our kinetic data would suggest that 2-methyltetrols in atmospheric particles are likely chemically stable against heterogeneous OH oxidation under humid conditions.

## 1. Introduction

The photochemical oxidation of isoprene is one of major sources of atmospheric secondary organic aerosols (SOA), which can potentially affect the regional and global air quality (Claeys et al., 2004; Carlton et al., 2009; Wennberg et al., 2018). In many aerosol source apportionment studies, 2-methyltetrols have been used as chemical tracers to quantify the contribution of isoprene-derived SOA to ambient particle organic mass (Kourtchev et al., 2005; Xia and Hopke, 2006; Lewandowski et al., 2007; Zhang et al., 2013; Xu et al., 2014; D'Ambro et al., 2017; He et al., 2018). While 2-methyltetrols are generally considered to be unreactive, this hypothesis has not been thoroughly tested. For instance, the heterogeneous oxidation of organic compounds present at particle surface by gas-phase oxidants such as hydroxyl (OH) radicals, ozone ( $\text{O}_3$ ) and nitrate radicals, has been shown to be efficient in

various laboratory and modeling studies (Rudich et al., 2007; George and Abbatt, 2010; Kroll et al., 2015; Chapleski et al., 2016; Estillore et al., 2016; Huang et al., 2018). Using the erythritol (Table 1) as a surrogate for 2-methyltetrols, Kessler et al. (2010) reported that heterogeneous oxidation of pure erythritol particles by gas-phase OH radicals with an effective OH uptake coefficient,  $\gamma_{\text{eff}}$ , of  $0.77 \pm 0.1$  and a corresponding chemical lifetime of  $\sim 13.8 \pm 1.4$  days at a relative humidity (RH) of 30 %. ~~Kessler et al. (2010) reported that pure erythritol particles can be heterogeneously oxidized by gas-phase OH radicals at a significant rate with an effective OH uptake coefficient,  $\gamma_{\text{eff}}$ , of  $0.77 \pm 0.1$  and a corresponding chemical lifetime of  $\sim 13.8 \pm 1.4$  days at a relative humidity (RH) of 30 %.~~ Hu et al. (2016) have investigated the heterogenous reactivity of ambient IEPOX-SOA (consisting of 2-methyltetrols, C5-alkene triols, organosulfate, etc.) towards gas-phase OH radicals in SE US and Amazon and reported the reaction kinetics for IEPOX-SOA based on the decay of  $\text{C}_5\text{H}_6\text{O}^+$  ion (a tracer ion for IEPOX-SOA in ambient particles) in their AMS measurements. They calculated on average a more than 2-week ( $19 \pm 9$  days) atmospheric lifetime of IEPOX-SOA against heterogeneous OH oxidation based on rate constant of  $4.0 \pm 2.0 \times 10^{-13} \text{ cm}^3 \text{ molecule}^{-1} \text{ s}^{-1}$  and averaged ambient OH concentration of  $1.5 \times 10^6 \text{ molecule cm}^{-3}$ . They also suggest that the observed rates may consider as a lower limit for individual molecular components of IEPOX-SOA (e.g. 2-methyltetrols) because it may take two or more OH reactions to make their AMS spectrum distinguishable from that of IEPOX-SOA after oxidation (Hu et al., 2016). These results suggest that the abundance of 2-methyltetrols reported in the literature and the amount of isoprene-derived SOA predicted using the chemical tracer method could be underestimated – if heterogeneous oxidation and other atmospheric removal processes (e.g. hydrolysis and aqueous-phase oxidation) have not been properly considered in aerosol source apportionment studies (Kessler et al., 2010).

To date, the heterogeneous kinetics and chemistry of many pure organic compounds or organic mixtures have been investigated (Zhang et al., 2015; Enami et al., 2016; Socorro et al., 2017; Marshall et al., 2018; Zhao et al., 2019). There remains large uncertainty on how inorganic salts alter the

heterogeneous kinetics and chemistry of organic compounds (McNeill et al., 2007, 2008; Dennis-Smith et al., 2012). A few recent laboratory studies have revealed that the presence of dissolved inorganic ions (e.g. ammonium sulfate, AS) can reduce the heterogeneous OH reactivity of organic compounds in aqueous organic-inorganic particles (e.g. methanesulfonic acid and 3-methylglutaric acid), but does not significantly alter the reaction mechanisms (Mungull et al., 2017; Kwong et al., 2018a; Lam et al., 2019a). In these studies, only a single inorganic-to-organic mass ratio was chosen to examine the impacts of the salts on the heterogeneous reactivity of organic compounds. However, organic compounds and inorganic salts often coexist with varying concentrations in the atmosphere. For instance, field studies have reported that the mass concentration of 2-methyltetrols ranges from 1-100's  $\text{ng m}^{-3}$  while that of AS ranges from few to tens  $\mu\text{g m}^{-3}$  (Schauer et al., 2002; Lewandowski et al., 2007; Kleindienst et al., 2010; Budisulistiorini et al., 2013; Xu et al., 2014; Hu et al., 2015). The mass concentration ratio of sulfate-to-2-methyltetrols can vary greatly from  $\sim 1.89$  to  $\sim 250$ . Since the impacts of the salts on the heterogeneous reactivity would depend on the relative abundance of organic compounds and inorganic salts, investigations on how the amount of the salts (or the inorganic-to-organic mass ratio) alters heterogeneous reactivity are necessary.

To gain more insights into the chemical transformation and stability of 2-methyltetrols in the atmosphere, experiments were conducted to investigate the heterogeneous OH oxidation of pure erythritol particles and particles containing erythritol and AS in different (water-free) inorganic-to-organic mass ratios (IOR or AS-to-erythritol mass ratio) at 85 % RH using an aerosol flow tube reactor (Table 1). The real-time chemical characterization of the particles before and after OH oxidation was carried out using a soft atmospheric pressure ionization source (Direct Analysis in Real Time, DART) coupled with a high-resolution mass spectrometer. Erythritol is chosen as a surrogate for investigating the heterogeneous reactivity of 2-methyltetrols (Kessler et al., 2010) while AS is chosen as a common atmospheric inorganic salt. We acknowledge that the IOR investigated in this work (IOR = 0.0–5.0) lies at the low range of IOR observed in atmospheric particles. This would better represent the

environments where the emission and photochemical activities of isoprene are significant. By examining the molecular evolution of pure erythritol particles and erythritol-AS particles during oxidation, we investigate how the presence and concentration of AS affects the heterogeneous OH kinetics and chemistry of erythritol. The results of this work will provide further insights into the chemical stability of 2-methyltetrols in atmospheric particles against heterogeneous OH oxidation.

## 2. Experimental Method

### 2.1 Heterogeneous Oxidation of Erythritol Particles and Erythritol-AS Particles

The heterogeneous OH oxidation of erythritol particles and erythritol-AS particles was investigated using an aerosol flow tube reactor at 20 °C and 85 % RH. Experimental details were given elsewhere (Cheng et al., 2016; Chim et al., 2017a, b; Lam et al., 2019a). Briefly, aqueous droplets were atomized using an atomizer and were directly mixed with ozone, oxygen (O<sub>2</sub>), dry nitrogen (N<sub>2</sub>), humidified N<sub>2</sub> and hexane before being introduced into the reactor. Inside the reactor, the particles were oxidized by gas-phase OH radicals, which were generated by the photolysis of ozone in the presence of ultraviolet light at 254 nm and water vapor. The gas-phase OH concentration was adjusted by varying the ozone concentration and was determined by measuring the change in the concentration of hexane before and after OH oxidation using a gas chromatograph coupled with a flame ionization detector (GC-FID) (Smith et al., 2009). The OH exposure, defined as the products of gas-phase OH concentration and particle residence time, was varied from 0.0 to  $\sim 2.29 \times 10^{12}$  molecule cm<sup>-3</sup> s in all experiments with the particle residence time of 90s.

After leaving the reactor, the ozone and gas-phase species in the particle stream were removed by passing through an annular Carulite catalyst denuder and an activated charcoal denuder, respectively, to allow the sampling of particle-phase products. A portion of the particle stream was then sampled by a scanning mobility particle sizer (SMPS) for particle size measurements. The remaining flow was directed to a stainless-steel tube heater, where the particles were fully vaporized in real time. The

resultant gas-phase species were then delivered into an ionization region. The erythritol particles and erythritol-AS particles were confirmed to be fully vaporized at 300 °C before introduced to the ionization region in separate experiments, thus yielding a mass spectrum representative of the entire particle (i.e., bulk composition). ~~The remaining flow was directed to a heater, where the particles were fully vaporized. In separate experiments, erythritol particles and erythritol AS particles were confirmed to be fully vaporized at 300 °C or above upon heating.~~ The gas-phase species leaving the heater were introduced into an atmospheric pressure ionization region, a narrow open space between the DART ionization source (IonSense: DART SVP), and the inlet orifice of the high-resolution mass spectrometer (Thermo Fisher, Q Exactive ~~Orbitrap~~ ~~Orbitrap~~Orbitrap) for real-time ionization and detection (Nah et al., 2013; Chan et al., 2013; 2014).

In the ionization region, the electrons ( $e^-$ ) produced by the Penning ionization of metastable He in the DART ionization source were captured by atmospheric  $O_2$  molecules to form anionic oxygen ions ( $O_2^-$ ) which then react with gas-phase species (Cody et al., 2005). Nah et al. (2013) have reported that erythritol can be detected as its deprotonated molecular ion,  $[M-H]^-$ , which can be formed via the proton abstraction from one of the hydroxyl groups of erythritol by  $O_2^-$ . As discussed later, carboxylic acids are likely formed upon oxidation and can be detected as  $[M-H]^-$  as well (Nah et al., 2013). The resultant ions were sampled by the high-resolution mass spectrometer and the particle-DART mass spectra were analyzed using the Xcalibur software (Thermo Fisher Scientific).

Control experiments were also carried out to investigate the effects of  $O_3$  and UV light on particles: one in the presence of  $O_3$  without the UV light and one in the presence of UV light without  $O_3$ . There were no significant changes in the DART-particle mass spectra in both control experiments for erythritol and erythritol-AS particles, indicating that the erythritol does not likely react with ozone and is not likely to be photolyzed. Additionally, no erythritol signal was observed when erythritol particles and erythritol-AS particles were removed from the particle stream by filtration using a particle filter

before entering the heater. This suggests the evaporation of erythritol was not significant under our experimental conditions, which agrees with the results reported by Kessler et al. (2010).

## 2.2 Physical State and Mixing Time Scale of Erythritol Particles

5 The physical state of particles can play a key factor in determining the composition, morphology and properties (e.g. viscosity) of the particles, which in turn influencing the heterogeneous reactivity (Renbaum and Smith, 2009; Slade and Knopf, 2014; Fan et al., 2015; Marshall et al., 2018; Karadima et al., 2019). Marsh et al. (2017) have measured the hygroscopicity of erythritol particles and found that erythritol particles are spherical droplets over their experimental RH range (60–100 %). Given the  
10 hygroscopic data and erythritol particles were always exposed to high RH (i.e. 85 %) and did not pass through a diffusion dryer in our system, they were likely aqueous droplets before oxidation. At low RH, erythritol particles are known to be viscous (Song et al., 2016; Grayson et al., 2017; Chu et al., 2018). With high particle viscosity, the diffusion of erythritol molecules from the bulk phase to the particle surface for oxidation slows down, and the overall heterogeneous reaction rate can be controlled  
15 by the diffusion (Chim et al., 2018; Marshall et al., 2018). To investigate whether particle viscosity affects the heterogeneous OH reactivity of erythritol particles at 85 % RH in this work, we calculated the characteristic time scale for diffusive mixing time ( $\tau_D$ ) of erythritol within the particle and that for gas phase OH–erythritol particle collisional timescale ( $\tau_{coll}$ ) (Chim et al., 2018). The  $\tau_D$  can be calculated as follow (Abbatt et al., 2012):

$$20 \quad \tau_D = \frac{D_p^2}{4D_{org} \pi^2} \quad (1)$$

where  $D_p$  is the mean surface-weighted diameter of erythritol particles ( $D_p = 276.1$  nm), and  $D_{org}$  is the diffusion coefficient of erythritol in the particle and can be estimated using the Stokes–Einstein Equation (Laguerie et al., 1976):

$$D_{org} = \frac{k_b T}{6\pi\eta R_H} \quad (2)$$

25 where  $D_{org}$  is the diffusion coefficient ( $\text{m}^2 \text{s}^{-1}$ ),  $k_b$  is the Boltzmann constant,  $T$  is the temperature,  $\eta$  is

the viscosity ( $\eta = 1.9 \times 10^{-3}$  Pa s at 293 K and 85 % RH) (Song et al., 2016), and  $R_H$  is the hydrodynamic radius of an erythritol molecule ( $R_H = 0.34 \pm 0.01$  nm) (Chu et al., 2018). Using Eq. 2,  $D_{org}$  is calculated to be  $3.54 \times 10^{-10}$  m<sup>2</sup> s<sup>-1</sup>, and the  $\tau_D$  is estimated to be  $5.45 \times 10^{-6}$  s at 85 % RH. The collision timescale between erythritol particles and gas-phase OH radicals,  $\tau_{coll}$ , can be estimated from the collision frequency ( $J_{coll}$ ) of gas-phase OH radicals on the particle surface (Chim et al., 2018):

$$J_{coll} \cong \frac{[OH] \overline{c_{OH}} A}{4} \quad (3)$$

where  $\overline{c_{OH}}$  is the mean thermal velocity of gas-phase OH radicals, and  $A$  is the surface area of the erythritol particle. Using Eq. 3,  $\tau_{coll}$  ( $= 1/J_{coll}$ ) is estimated to be about  $2.36 \times 10^{-6}$  s at the maximum OH exposure (i.e. highest gas-phase OH concentration). In this study, as the diffusive mixing time scale ( $\tau_D = 5.45 \times 10^{-6}$  s) and OH-particle collisional timescale ( $\tau_{coll} = 2.36 \times 10^{-6}$  s) are estimated to be in the same order of magnitude, erythritol could be reasonably assumed to be well-mixed within the particles under our experimental conditions.

### 2.3 Physical State and Mixing Time Scale of Erythritol–AS Particles

Organic compounds and inorganic salts usually coexist in atmospheric particles. In response to atmospheric conditions (e.g. RH and temperature) and particle composition, these mixed particles can undergo phase transition (deliquescence and crystallization) and phase separation (e.g. solid-liquid and liquid-liquid phase separation) (Braban and Abbatt, 2004; Song et al., 2012a, b; You et al., 2013, 2014; Veghte et al., 2014; Karadima et al., 2019). Laboratory studies have reported that no phase separation was observed for organic–inorganic particles when organic compounds with O/C ratio larger than 0.8. Although the physical state of erythritol–AS particles has not been experimentally measured, erythritol–AS particles are likely aqueous droplets at high RH (i.e. 85 % RH) and exists as a single aqueous phase prior to oxidation as erythritol has an O/C ratio of one (Table 1). To our best knowledge, the viscosity of erythritol–AS particles with different IOR has not been reported in the literature. However, for the purposes of this work we will assume that erythritol is well mixed within all



erythritol–AS particles prior to oxidation under our experimental conditions.

### 3. Results and Discussions

#### 3.1 Particle-DART Mass Spectra of Erythritol and Erythritol–AS Particles

5 The particle-DART mass spectra of erythritol and erythritol–AS particles with different IORs before and after OH oxidation are shown in Figure 1. For erythritol particles, before oxidation, only one major peak of the deprotonated molecular ion of erythritol ( $\text{C}_4\text{H}_9\text{O}_4^-$ ) at  $m/z$  111 is observed, together with some small background peaks. After oxidation, at the highest OH exposure, unreacted erythritol has the largest signal and accounts for 27.8 % of the total ion signal. Two major product peaks evolve. The  
10  $\text{C}_4$  functionalization products ( $\text{C}_4\text{H}_8\text{O}_5$ ) and  $\text{C}_3$  fragmentation products ( $\text{C}_3\text{H}_6\text{O}_4$ ) contribute 23.4 % and 17.9 % of the total ion signal, respectively. Some small product peaks ( $\text{C}_4\text{H}_7\text{O}_4^-$ ,  $\text{C}_4\text{H}_5\text{O}_4^-$ ,  $\text{C}_4\text{H}_3\text{O}_4^-$  and  $\text{C}_3\text{H}_5\text{O}_3^-$ ) are also detected.

The particle-DART mass spectra of erythritol–AS particles are very similar to that of erythritol  
15 particles, except for an inorganic sulfate peak. Before oxidation, there are two major peaks at  $m/z$  97 and  $m/z$  111, corresponding to the bisulfate ion ( $\text{HSO}_4^-$ ) and the deprotonated molecular ion of erythritol ( $\text{C}_4\text{H}_9\text{O}_4^-$ ), respectively. After oxidation, the  $\text{C}_4$  functionalization products ( $\text{C}_4\text{H}_8\text{O}_5$ ) and  $\text{C}_3$  fragmentation products ( $\text{C}_3\text{H}_6\text{O}_4$ ) are the two major products together with some minor product peaks.

The  $\text{HSO}_4^-$  likely originated from AS. Before introduced to the ionization region, erythritol–AS  
20 particles were fully vaporized under high temperature and may thus thermally decompose into gas-  
phase  $\text{NH}_3$  and  $\text{H}_2\text{SO}_4$  (Drewnick et al., 2015), which can be detected as  $\text{HSO}_4^-$  via direct ionization  
(Hajslova et al., 2011; Lam et al., 2019a, b; Kwong et al., 2018a, b). The intensity of  $\text{HSO}_4^-$  before  
and after oxidation (Figure S1, *supplementary material*) showed no significant change, which is  
consistent with the argument in previous studies (Cooper and abbatt, 1996; Anastasio and Newberg,  
25 2007) that the surface reaction between dissolved sulfate ions and gas-phase OH radicals is not efficient.  
The  $\text{HSO}_4^-$  is likely originated from AS. For the erythritol–AS particles, AS dissociates into the

ammonium and sulfate ions. Upon heating and evaporation, the particles becomes acidified by the evaporative loss of ammonia into gas phase and the dissolved sulfate ions can be detected as  $\text{HSO}_4^-$  via direct ionization (Hajslova et al., 2011; Lam et al., 2019a, b; Kwong et al., 2018a, b). The intensity of  $\text{HSO}_4^-$  before and after oxidation (Figure S1, *supplementary material*) had no significant change, which is consistent with the argument made by George and Abbatt (2010) that the surface reaction between dissolved ions and gas-phase OH radicals is not efficient. As same reaction products are observed for both erythritol particles and erythritol-AS particles with different IORs, these results suggest that the heterogenous OH reaction mechanisms of erythritol do not significantly affect by the presence and amount of AS.

As shown in Figure 1, the deprotonated molecular ion of erythritol is the dominant peak in the mass spectra before oxidation, suggesting that the thermal decomposition of erythritol might not be significant. These results are consistent with the literature (Nah et al., 2013). Nah et al. (2013) have also showed that the deprotonated molecular ions are the dominant ions for carboxylic acids in their particle-DART analysis. Taken together, these results indicate that the effect of thermal decomposition on the observed products may be insignificant. However, we would like to note that some possible reaction products (e.g. organic peroxides and oligomers) could be formed from reactions between peroxy radicals (Stark et al., 2017). We do not rule out the formation of these products upon OH oxidation of erythritol as they may undergo thermal decomposition at high temperature with the cleavage of O-O bond (Mukundan and Kishore, 1990). Further investigation on the formation of organic peroxides and oligomers upon heterogeneous OH oxidation of organic compounds is desirable. However, we would like to note that some possible reaction products (e.g. organic peroxides and oligomers) could be formed from reactions between peroxy radicals) may thermally decompose (Stark et al., 2017). We do not rule out the formation of these products upon OH oxidation of erythritol, but there was no indication of fragment ions expected from the thermal decomposition of these products in the particle DART mass spectra. Further investigation on the formation of these products during

~~heterogeneous OH oxidation of organic compounds is desirable.~~ In the following, the heterogeneous OH kinetics and chemistry of the erythritol and erythritol-AS particles is examined based on the particle-DART mass spectra measured at different extent of oxidation.

### 5 3.2 Oxidation Kinetics of Erythritol and Erythritol-AS Particles

Figure 2a shows the normalized decay of erythritol in erythritol particles and erythritol-AS particles with different IOR as a function of OH exposure. For all these particles, the OH-initiated decay of erythritol exhibits an exponential trend and can be fit with an exponential function:

$$\ln \frac{I}{I_0} = -k [OH] \cdot t \quad (4)$$

10 where  $I$  is the signal intensity of erythritol at a given OH exposure,  $I_0$  is the signal intensity before oxidation,  $k$  is the effective second-order heterogeneous OH rate constant, and  $[OH] \cdot t$  is the OH exposure. It can be seen that the rate of reaction decreases with decreasing amount of erythritol or increasing amount of AS (Table 1). When the IOR increases from 0.0 to 5.0, the  $k$  decreases from  $5.39 \pm 0.12 \times 10^{-13}$  to  $1.56 \pm 0.04 \times 10^{-13} \text{ cm}^3 \text{ molecule}^{-1} \text{ s}^{-1}$ . Further, the initial effective OH uptake  
15 coefficient,  $\gamma_{\text{eff}}$ , defined as the fraction of OH collisions with erythritol molecule that result in a reaction, can be computed (Kessler et al., 2010; Davies and Wilson, 2015),

$$\gamma_{\text{eff}} = \frac{2 D_p \rho mfs N_A k}{3 M \overline{c_{OH}}} \quad (5)$$

where  $D_p$  is the mean surface-weighted particle diameter before OH oxidation,  $\rho$  is the particle density before oxidation,  $N_A$  is the Avogadro's number,  $mfs$  is the mass fraction of erythritol,  $M$  is the molecular weight of erythritol, and  $\overline{c_{OH}}$  is the average speed of gas-phase OH radicals. For erythritol particles, the initial mean surface-weighted particle diameter was 276.1 nm and decreased to 255.8 nm after oxidation (~ 7.3 %). ~~For erythritol particles, before oxidation, the mean surface-weighted particle diameter was 276.1 nm.~~ The density of erythritol particles is estimated to be  $1.173 \text{ g cm}^{-3}$ , using the volume additivity rule with the density of water and erythritol ( $1.451 \text{ g cm}^{-3}$ ) and particle composition  
20 (i.e. mass fraction of solute,  $mfs$ ). The  $mfs$  is derived from the hygroscopicity data reported by Marsh  
25

et al. (2017) and is reported to be  $0.47 \pm 0.02$  at 85 % RH, which agrees well with model simulations ( $mfs = 0.482$ ) using the Aerosol Inorganic–Organic Mixtures Functional groups Activity Coefficients (AIOMFAC) model (Zuend et al., 2008; Zuend et al., 2011). For erythritol–AS particles, the particle diameters were measured to be 278.2–281.5 nm before oxidation (Table 1). Slight decreases in particle diameter ( $\sim 5.8\%$ ,  $\sim 4.9\%$ ,  $\sim 2.6\%$  at IOR = 0.5, 1.0 and 5.0, respectively) were also observed (Figure S2, supplementary material). ~~For erythritol–AS particles, the particle diameters were measured to be 278.2–281.5 nm before oxidation.~~ The  $mfs$  of erythritol in erythritol–AS particles are obtained from the model simulation using AIOMFAC to be 0.280, 0.210, 0.061 at IOR = 0.5, 1.0 and 5.0, respectively (Table 1). Based on the composition of erythritol–AS particles (i.e.  $mfs$ ), the particle density was also estimated using the volume additivity rule with the density of water, erythritol and AS ( $1.77 \text{ g cm}^{-3}$ ). Using Eq. 5, the  $\gamma_{\text{eff}}$  is calculated to be  $0.45 \pm 0.025$  for erythritol particles (i.e. IOR = 0). For erythritol–AS particles, the  $\gamma_{\text{eff}}$  is calculated to be  $0.20 \pm 0.010$ ,  $0.12 \pm 0.006$ ,  $0.02 \pm 0.001$  at IOR = 0.5, 1.0 and 5.0, respectively. Figure 2b shows that the heterogeneous reactivity of erythritol toward gas-phase OH radicals as a function of IOR at 85 % RH. The  $\gamma_{\text{eff}}$  is found to decrease from  $0.45 \pm 0.025$  to  $0.02 \pm 0.001$  when the IOR increases from 0.0 to 5.0. We acknowledge that the span of polydisperse particles could have effects on the determination of  $\gamma_{\text{eff}}$ . Further study which measures the  $\gamma_{\text{eff}}$  for size selected monodisperse and polydisperse particles is desired to better investigate the effect of particle size distribution on  $\gamma_{\text{eff}}$  calculation. ~~The  $\gamma_{\text{eff}}$  is found to decrease from  $0.45 \pm 0.025$  to  $0.02 \pm 0.001$  when the IOR increases from 0.0 to 5.0.~~

These results agree with the literature that the addition of AS decreases the overall rate of heterogeneous OH oxidation with organic compounds (Mungull et al., 2017; Kwong et al., 2018a; Lam et al., 2019a). We carried out molecular dynamics (MD) simulations to gain a better insight into the effect of dissolved ions on the heterogeneous OH reactivity of erythritol. The details of MD simulation are given in the *supplementary material*. Previous simulation results suggest excess kinetic energy that an impinging gas molecule may carry will dissipate in a few ps after collision (Vieceli et

al., 2005; Li et al., 2019). The difference between this very short timescale and the experimental timescale of the reaction on ms timescale indicates that the reaction is not likely initiated by the direct collision between the gas-phase OH radical and the erythritol molecule present at the particle surface. Our simulation also shows that it is not easy for the gas-phase OH radical to collide near an erythritol molecule at first impact with or without salt. With salt, the probability for the gas-phase OH radical to collide near an erythritol molecule becomes even lower because of lower concentrations as shown in Figure S3S3, suggesting the reaction via direct impact is unlikely.

Some gas-phase OH radicals would be absorbed by the particle after collision, and the reaction would require an absorbed OH radical and an erythritol to meet many times by diffusion before the reaction could happen. To shed light on how likely absorbed OH radical meets erythritol within the droplet, the probability densities of the distance between the centers of mass (COMs) of the OH radical and the closest erythritol molecule in presence and in absence of salt were calculated. As shown in Figure S2S4, in the presence of (hygroscopic) salt, the erythritol-AS particle contains more water and the concentrations of erythritol and adsorbed OH radical are smaller, making the average distance between the OH radical and its nearest erythritol longer relative to pure erythritol particle. The longer average distance would slow down the reaction rate, which is consistent with the decreased reaction rate in the experiment in the presence of salt.

Another possibility for this lower heterogeneous reactivity might due to the change in surface-bulk partitioning behavior of organic compound in the presence of AS which could potentially alter the surface concentration of organic reactant. Previous studies have found that the addition of AS could resulted in a pronounced increase/decrease in particle surface tension compared to that of organic/water particle, indicating a salting in/out effect (Ekström et al., 2009; Zhang and Carloni, 2012; Boyer and Dutcher, 2017; Fan et al., 2019). These effects might result in smaller/larger surface concentration of organic than that in the bulk and further affect the overall reactivity. To our best knowledge, the surface-

bulk-partitioning behavior of erythritol molecules in the presence of AS has not been experimentally measured. Ekström et al. (2009) have measured the surface tension using a FTÅ 125 tensiometer and have reported that when AS was mixed with 2-methylerythritol (with chemical structures similar to erythritol), the surface tension,  $\sigma$  was found to increase compared to that of 2-methylerythritol. For instance, for the system with 17 wt % of AS and 0.05 M of 2-methylerythritol, the surface tension was  $\sim 72.6 \text{ mN m}^{-1}$ , which is larger than that for 2-methylerythritol/water system ( $\sigma (0.05 \text{ M}) = \sim 69.7 \text{ mN m}^{-1}$ ). In their study, the surface tension increased from  $\sim 50.3 \text{ mN m}^{-1}$  to  $72.6 \text{ mN m}^{-1}$  when IOR increased from  $\sim 0.8$  to  $\sim 25.0$ , suggesting a salting in effect. On the other hand, Riva et al. (2019) have recently observed an interfacial tension depression using a biphasic microfluidic platform when AS was mixed with 2-methyltetrols (1.55 M of AS and 0.37 M of 2-methyltetrols (IOR =  $\sim 4.1$ )), suggesting a salting out effect. Based on these two results, the salt effect on the surface-bulk-partitioning behavior of 2-methyltetrols and likely erythritol remains unclear. Future investigations which can well represent the distribution of erythritol molecules at the particle surface are desirable to better understand how the presence of salts would alter the surface concentration of organic molecule and ultimately affect its heterogeneous reactivity. For instance, the smaller surface concentration of reactive species could ultimately lower the reactive collision probability between the organic compound and OH radicals, slowing down the overall heterogeneous oxidation rate. While our model simulations could not provide the density profile of erythritol molecules within particles, future investigations are desirable to better understand how the concentration of organic molecule at the particle surface would affect the heterogeneous reactivity in the presence and absence of the salt.

Based on the kinetic data, we also estimate the chemical lifetime of erythritol against heterogeneous OH oxidation,  $\tau$  under different particle composition (i.e. IOR) at 85 % RH (Kroll et al., 2015):

$$\tau = \frac{[\text{Erythritol}]}{d[\text{Erythritol}]/dt} = \frac{1}{k[\text{OH}]} \quad (6)$$

As shown in Table 1, assuming a 24 h averaged OH concentration of  $1.5 \times 10^6 \text{ molecule cm}^{-3}$  (Mao et

al., 2009), the  $\tau$  of pure erythritol particles is estimated to be  $14.7 \pm 0.33$  days. The timescales are slightly longer than those of other important particle removal processes, such as dry and wet deposition ( $\sim 5$ – $12$  days) with the similar particle size (200 nm) (Kanakidou et al., 2005). A similar result has been reported in the literature. Kessler et al. (2010) have investigated the heterogeneous OH oxidation of pure erythritol particles at a lower RH (30 % RH) and reported a chemical lifetime of about  $13.8 \pm 1.4$  days. These results suggest that the variation of RH does not significantly alter the rate of OH reaction with erythritol. On the other hand, the reaction rates depend on the concentration of erythritol and AS. The chemical lifetime increases from  $14.7 \pm 0.33$  days to  $49.5 \pm 1.43$  days when the IOR increases from 0.0 to 5.0 (Table 1). These indicate that erythritol become more chemically stable against OH oxidation when the salt is present. We acknowledge that the highest IOR investigated in this work (IOR = 5.0) lies at the low range of IOR reported for the 2-methyltetrols in atmospheric particles. The results of this work might provide insights into how 2-methyltetrols chemically age through heterogeneous OH oxidation in the environments where the emission and photochemical activities of isoprene are significant. We also note that 2-methyltetrols is often mixed with a large amount of AS and the ambient IOR can be as large as  $\sim 250$ . Since the heterogeneous reactivity decreases with increasing IOR, large ambient IOR values may suggest that the heterogeneous OH reactivity of 2-methyltetrols in atmospheric particles would be much slower than previously predicted based on experiments with pure organic particles. It would be reasonable to assume that 2-methyltetrols are likely chemically stable against heterogeneous OH oxidation over their atmospheric timescales.

### 3.3 Proposed Reaction Mechanisms

As shown in Figure 1, same reaction products are observed for both erythritol and erythritol–AS particles, suggesting the presence and the amount of AS does not significantly affect the formation pathways of major reaction products. We tentatively propose the same reaction pathways for OH reaction with erythritol in the absence and presence of AS based on particle-phase reactions previously reported in the literature (Bethel et al., 2003; Kessler et al., 2010; George and Abbatt, 2010; Kroll et

al., 2015). As shown in Scheme 1, OH oxidation with erythritol can be initiated by the hydrogen abstraction from the two C–H bonds (Path A and Path B) and two O–H bonds (Path C and Path D). A variety of functionalization (Section 3.3.1) and fragmentation products (Section 3.3.2) can be formed when gas-phase OH radicals attack different reaction sites.

5

### 3.3.1 Functionalization Products

Scheme 1 shows a variety of functionalization products can be possibly formed during oxidation. The formation of functionalization products is likely originated from the hydrogen abstraction occurred at the C–H bonds (Scheme 1: Path A and Path B). This is because when the hydrogen abstraction occurs  
10 on the O–H groups (Scheme 1: Path C and Path D), the resultant alkoxy radicals tend to decompose into smaller fragmentation products.

**C<sub>4</sub>H<sub>8</sub>O<sub>5</sub>** As shown in Scheme 1 (Path A), the major C<sub>4</sub> functionalization product (C<sub>4</sub>H<sub>8</sub>O<sub>5</sub>), as shown in Figure 1, can be formed when the hydrogen abstraction occurs at the secondary carbon site. At the  
15 first oxidation step, an alkyl radical is formed after hydrogen abstraction by OH radicals and quickly reacts with an oxygen molecule to form a peroxy radical. The self-reactions of two peroxy radicals can produce the C<sub>4</sub> carboxylic acid (C<sub>4</sub>H<sub>8</sub>O<sub>5</sub>) via well-known particle-phase reactions such as Russell and Bennett and Summers reactions (Russell, 1957; Bennett and Summers, 1973). While a carboxylic acid group is formed during oxidation, the effective saturation vapor pressure, *C*\* of the C<sub>4</sub> carboxylic acid  
20 is estimated to be 0.195 μg m<sup>-3</sup> using the saturation vapor pressure predicted by EVAPORATION (Compernelle et al., 2011). Given its low volatility, it likely remains in particle phase upon production.

**C<sub>4</sub>H<sub>8</sub>O<sub>4</sub>** A small peak has been observed for another C<sub>4</sub> functionalization products (C<sub>4</sub>H<sub>8</sub>O<sub>4</sub>) (Figure 1). The formation of these products could be originated from the unimolecular HO<sub>2</sub> elimination of  
25 hydroxyperoxy radicals (Bothe et al., 1983; Bethel et al., 2003; Kessler et al., 2010). For instance, when the hydrogen abstraction occurs at the secondary carbon site (Scheme 1: Path A), a



hydroxyperoxy radical can undergo the unimolecular HO<sub>2</sub> elimination process to form a C<sub>4</sub> hydroxyaldehyde (C<sub>4</sub>H<sub>8</sub>O<sub>4</sub>). Moreover, when the hydrogen abstraction occurs at the tertiary carbon site (Scheme 1: Path B), a C<sub>4</sub> hydroxyketone (C<sub>4</sub>H<sub>8</sub>O<sub>4</sub>) can be formed via the same process. This unimolecular HO<sub>2</sub> elimination process is expected to be kinetically favorable for polyols (Bothe et al., 1978a, b). This is because the hydroxyl group adjacent to the peroxy group can stabilize the resultant carbonyl group by forming strong intramolecular hydrogen bond, thus enhancing the unimolecular HO<sub>2</sub> elimination rate (Bothe et al., 1978a, b; Cheng et al., 2016). As show in Figure 1, the ion signal intensity of these functionalization products is only less than 5 % of the total ion signal. Although the ionization efficiencies of these products were not corrected in this study, our earlier study found that the ionization efficiency of ketone products is higher than alcohol products with same carbon number during the DART ionization processes (Chan et al., 2014). Thus the low abundance of the ketone/aldehyde products might be better attributed to the high volatilities of these functionalization products. When the unimolecular HO<sub>2</sub> elimination occurs, a hydroxyl group is being converted into a carbonyl group. This increases the volatilities of reaction products compared to their parent compounds. For instance, the C\* of the C<sub>4</sub> hydroxyketone (Scheme 1: Pathway B) and the C<sub>4</sub> hydroxyaldehyde (Scheme 1: Pathway A) is estimated to be  $3.01 \times 10^2 \mu\text{g m}^{-3}$  and  $6.95 \times 10^2 \mu\text{g m}^{-3}$ , respectively. The volatilities of these two products are predicted to be about 1–2 orders of magnitude larger than that of pure erythritol ( $C^* = 5.71 \mu\text{g m}^{-3}$ ).

### 3.3.2 Fragmentation Products

**C<sub>3</sub>H<sub>6</sub>O<sub>4</sub>** Fragmentation products can be generated from the decomposition of alkoxy radicals during oxidation. The major C<sub>3</sub> fragmentation product is likely originated from the hydrogen abstraction at the tertiary carbon site (Scheme 1: Pathway B). The alkoxy radicals resulted from peroxy-peroxy reactions can fragment to form a C<sub>2</sub> hydroxyketone (C<sub>2</sub>H<sub>4</sub>O<sub>2</sub>) and a C<sub>3</sub> carboxylic acid (C<sub>3</sub>H<sub>6</sub>O<sub>4</sub>). The C<sub>2</sub> hydroxyketone is volatile ( $C^* = 3.75 \times 10^7 \mu\text{g m}^{-3}$ ) and likely partitions back to the gas phase. For the C<sub>3</sub> carboxylic acid, although a carbon atom is lost, the formation of the carboxylic acid functional

group lowers its volatility ( $C^* = 5.64 \mu\text{g m}^{-3}$ ). Thus, it is expected to be nonvolatile and likely remains in the particle phase. Additionally, the structure–activity relationship (SAR) model developed for the decomposition of alkoxy radicals suggests that the formation of the larger fragmentation product (i.e.  $\text{C}_3$  carboxylic acid) is more kinetically favorable than that of the smaller fragmentation product (i.e.  $\text{C}_2$  hydroxyketone) upon decomposition as the formation rate coefficient ( $k_{\text{SAR}}$ ) of the  $\text{C}_3$  fragmentation product is  $7.13 \times 10^{12} \text{ s}^{-1}$ , which is about three order of magnitude higher than that of the  $\text{C}_2$  fragmentation product ( $3.40 \times 10^9 \text{ s}^{-1}$ ) (Peeters et al., 2004; Vereecken et al., 2009).

During oxidation, a number of fragmentation products can be possibly formed. However, the ion signals of these fragmentation products that remained in the particle phase are very small or not detected in the particle-DART mass spectra (Figure 1). This might attribute to the volatilization of these fragmentation products. For instance, when the hydrogen abstraction occurs at the secondary carbon site (Scheme 1: Path A), the decomposition of the alkoxy radical yields a formic acid ( $\text{HCOOH}$ ) ( $C^*$  of  $1.90 \times 10^7 \mu\text{g m}^{-3}$ ). Alkoxy radicals can be directly formed when the hydrogen abstraction occurs at the two OH-groups (Scheme 1: Path C and Path D). The decomposition of resultant alkoxy radicals can yield volatile fragmentation products such as  $\text{HCOOH}$ , a  $\text{C}_3$  hydroxyaldehyde ( $\text{C}_3\text{H}_6\text{O}_3$ ,  $C^* = 1.75 \times 10^5 \mu\text{g m}^{-3}$ ) and a  $\text{C}_2$  hydroxyketone ( $\text{C}_2\text{H}_4\text{O}_2$ ,  $C^* = 3.75 \times 10^7 \mu\text{g m}^{-3}$ ). These products likely partition back to the gas phase due to their high volatilities.

Overall, the formation of two major products detected in the particle-DART mass spectra (Figure 1) is likely originated from two distinct reaction sites. The major functionalization products ( $\text{C}_4$  carboxylic acid) are likely formed when the hydrogen abstraction occurs at the secondary carbon site followed by functionalization processes (Scheme 1: Path A), while the major fragmentation product ( $\text{C}_3$  carboxylic acid) are likely formed from the decomposition of an alkoxy radical formed at the tertiary carbon site (Scheme 1: Path B). Further investigations on the DART ionization efficiency and detection of both particle-phase and gas-phase products are highly desirable to better understand the reaction

mechanisms and assess the relative importance between functionalization, fragmentation and volatilization processes in governing the composition of erythritol particles during heterogeneous OH oxidation.

#### 5    **4. Conclusions and Atmospheric Implications**

To date, there remains considerable uncertainty in how inorganic salts alter the heterogeneous reactivity of organic compounds, which ultimately governs the chemical lifetime of organic compounds in the atmosphere. Here, we investigated the effects of AS on the kinetics, products and mechanisms upon heterogeneous OH oxidation of erythritol at 85 % RH at different (dry) mass ratios of erythritol and AS. Particle-DART mass spectra obtained for both erythritol and erythritol-AS particles showed the same reaction products, suggesting that formation pathways of major reaction products do not significantly affect by the presence and amount of AS. On the other hand, the heterogeneous reactivity of erythritol toward gas-phase OH radicals could be slower in erythritol-AS particles compared to pure erythritol particles, depending on the concentration of erythritol and AS. This could be explained by that the colliding probability between OH radical and erythritol in the particle and at the particle surface become lower in the presence of salts, resulting in a smaller overall reaction rate. Overall, our results provide evidence that inorganic salts likely alter the heterogeneous reactivity of organic compounds with gas-phase OH radicals rather than the reaction mechanisms. Further, our kinetic data suggest that given the ambient concentration of 2-methyltetrols and AS reported in field measurements, 2-methyltetrols in the atmospheric particles are likely chemical stable against heterogeneous OH oxidation under humid conditions.

25    Recent studies have shown that the phase state and viscosity of the particles depending on the particle composition and environmental factors can significantly affect the diffusivity of organic molecules.

water molecules and oxidants such as gas-phase OH radicals, which in turn the overall oxidation rate and formation of products (Chan et al., 2014; Slade and Knopf, 2014; Chim et al., 2017a; Marshall et al., 2016; 2018). Isoprene-derived SOA, especially when formed in the presence of acidic sulfate particles have been reported to be highly viscous (Shrivastava et al., 2017; Olson et al., 2019; Zhang et al., 2019). For instance, Riva et al. (2019) have shown that a viscous IEPOX-SOA coating was likely formed in the presence of acidic sulfate seed particles. The diffusion of organic molecules (e.g. 2-methyltetrols) from the bulk to the particle surface could slow down, lowering the overall heterogeneous reactivity.

To date, the effects of the complex interplay between particle phase, morphology and viscosity on the heterogeneous reactivity remains largely unexplored. We would like to acknowledge that in this study the rate constants and lifetimes measured for well mixed erythritol particles and erythritol-AS particles at a high RH may consider as an upper limit. The OH oxidation of 2-methyltetrols in ambient particles could be slower than our reported values, depending on the formation pathways and composition of IEPOX-SOA and atmospheric conditions (e.g. RH and temperature). All these results suggest that a single kinetic parameter may not be well described for the heterogeneous OH oxidation erythritols and 2-methyltetrols in atmosphere since the rates can vary significantly, depending on the particle composition, phase and morphology and environmental factors.

#### **Data availability**

The underlying research data are available upon request from the corresponding author (mnchan@cuhk.edu.hk).

#### **Author contributions**

Rongshuang Xu and Man Nin Chan designed and ran the experiments. Rongshuang Xu, Hoi Ki Lam, and Man Nin Chan prepared the manuscript. All co-authors provided comments and suggestions to the

manuscript.

### Competing interests

The authors declare that they have no conflict of interest.

5

### Acknowledgements

Rongshuang Xu, Hoi Ki Lam and Man Nin Chan are supported by the Hong Kong Research Grants Council (HKRGC) Project ID: 2130626 (Ref 14300118). Kevin R. Wilson is supported by the Department of Energy, Office of Science, Office of Basic Energy Sciences, Chemical Sciences,  
10 Geosciences, and Biosciences Division under Contract No. DE-AC02-05CH11231.

### References

- Anastasio, C. and Newberg, J. T.: Sources and sinks of hydroxyl radical in sea-salt particles, J. Geophys. Res.: Atmos., 112, doi:10.1029/2006jd008061, 2007.
- 15 Bertram, A. K., Martin, S. T., Hanna, S. J., Smith, M. L., Bodsworth, A., Chen, Q., Kuwata, M., Liu, A., You, Y. and Zorn, S. R.: Predicting the relative humidities of liquid-liquid phase separation, efflorescence, and deliquescence of mixed particles of ammonium sulfate, organic material, and water using the organic-to-sulfate mass ratio of the particle and the oxygen-to-carbon elemental ratio of the organic component, Atmos. Chem. Phys., 11, 10995–11006, doi:10.5194/acp-11-10995-2011, 2011.
- 20 Bennett, J. E. and Summers, R.: Product studies of the mutual termination reactions of sec-alkylperoxy radicals: evidence for non-cyclic termination, Can. J. Chem., 52, 1377–1379, doi:10.1139/v74-209, 1974.
- Bethel, H. L., Atkinson, R. and Arey, J.: Hydroxycarbonyl products of the reactions of selected diols with the OH radical, J. Phys. Chem. A, 107, 6200–6205, doi:10.1021/jp027693l, 2003.

- Bothe, E., Schuchmann, M. N., Schulte-Frohlinde, D. and Sonntag, C. V.: HO<sub>2</sub> elimination from  $\alpha$ -hydroxyalkylperoxyl radicals in aqueous solution, *Photochem. Photobiol.*, 28, 639–643, doi:10.1111/j.1751-1097.1978.tb06984.x, 1978a.
- Bothe, E., Schulte-Frohlinde, D. and Sonntag, C. V.: Radiation chemistry of carbohydrates. Part 16. Kinetics of HO<sub>2</sub> elimination from peroxyl radicals derived from glucose and polyhydric alcohols, *J. Chem. Soc., Perkin Trans. 2*, 416, doi:10.1039/p29780000416, 1978b.
- Bothe, E., Schuchmann, M. N., Schulte-Frohlinde, D. and Sonntag, C. V.: Hydroxyl radical-induced oxidation of ethanol in oxygenated aqueous solutions. a pulse radiolysis and product study, *Zeitschrift für Naturforschung B*, 38, 212–219, doi:10.1515/znb-1983-0218, 1983.
- Boyer, H. C., and Dutcher, C. S.: Atmospheric aqueous aerosol surface tensions: isotherm-based modeling and biphasic microfluidic measurements. *J. Phys. Chem. A*, 121, 4733–4742. doi:10.1021/acs.jpca.7b03189, 2017.
- Braban, C. F. and Abbatt, J. P. D.: A study of the phase transition behavior of internally mixed ammonium sulfate - malonic acid aerosols, *Atmos. Chem. Phys.*, 4, 1451–1459, doi:10.5194/acp-4-1451-2004, 2004.
- Budisulistiorini, S. H., Canagaratna, M. R., Croteau, P. L., Marth, W. J., Baumann, K., Edgerton, E. S., Shaw, S. L., Knipping, E. M., Worsnop, D. R., Jayne, J. T., Gold, A. and Surratt, J. D.: Real-time continuous characterization of secondary organic aerosol derived from isoprene epoxydiols in downtown Atlanta, Georgia, using the aerodyne aerosol chemical speciation monitor, *Environ. Sci. Technol.*, 47, 5686–5694, doi:10.1021/es400023n, 2013.
- Carlton, A. G., Wiedinmyer, C. and Kroll, J. H.: A review of secondary organic aerosol (SOA) formation from isoprene, *Atmos. Chem. Phys.*, 9, 4987–5005, doi:10.5194/acp-9-4987-2009, 2009.
- Chan, M. N., Surratt, J. D., Claeys, M., Edgerton, E. S., Tanner, R. L., Shaw, S. L., Zheng, M., Knipping, E. M., Eddingsaas, N. C., Wennberg, P. O. and Seinfeld, J. H.: Characterization and quantification of isoprene-derived epoxydiols in ambient aerosol in the southeastern united states, *Environ. Sci. Technol.*, 44, 4590–4596, doi:10.1021/es100596b, 2010.

- Chan, M. N., Nah, T. and Wilson, K. R.: Real time in situ chemical characterization of sub-micron organic aerosols using Direct Analysis in Real Time mass spectrometry (DART-MS): the effect of aerosol size and volatility, *The Analyst*, 138, 3749, doi:10.1039/c3an00168g, 2013.
- Chan, M. N., Zhang, H., Goldstein, A. H. and Wilson, K. R.: Role of water and phase in the heterogeneous oxidation of solid and aqueous succinic acid aerosol by hydroxyl radicals, *J. Phys. Chem. C*, 118, 28978–28992, doi:10.1021/jp5012022, 2014.
- Cheng, C. T., Chan, M. N. and Wilson, K. R.: Importance of unimolecular HO<sub>2</sub> elimination in the heterogeneous OH reaction of highly oxygenated tartaric acid aerosol, *J. Phys. Chem. A*, 120, 5887–5896, doi:10.1021/acs.jpca.6b05289, 2016.
- Chim, M. M., Chow, C. Y., Davies, J. F. and Chan, M. N.: Effects of relative humidity and particle phase water on the heterogeneous OH oxidation of 2-methylglutaric acid aqueous droplets, *J. Phys. Chem. A*, 121, 1666–1674, doi:10.1021/acs.jpca.6b11606, 2017a.
- Chim, M. M., Cheng, C. T., Davies, J. F., Berkemeier, T., Shiraiwa, M., Zuend, A. and Chan, M. N.: Compositional evolution of particle-phase reaction products and water in the heterogeneous OH oxidation of model aqueous organic aerosols, *Atmos. Chem. Phys.*, 17, 14415–14431, doi:10.5194/acp-17-14415-2017, 2017b.
- Cooper, P. L. and Abbatt, J. P. D.: Heterogeneous Interactions of OH and HO<sub>2</sub> Radicals with Surfaces Characteristic of Atmospheric Particulate Matter, *J. Phys. Chem.*, 100, 2249–2254, doi:10.1021/jp952142z, 1996.
- Chim, M. M., Lim, C. Y., Kroll, J. H. and Chan, M. N.: Evolution in the reactivity of citric acid toward heterogeneous oxidation by gas-phase OH radicals, *ACS Earth Space Chem.*, 2, 1323–1329, doi:10.1021/acsearthspacechem.8b00118, 2018.
- Chu, Y., Evoy, E., Kamal, S., Song, Y. C., Reid, J. P., Chan, C. K. and Bertram, A. K.: Viscosity of erythritol and erythritol–water particles as a function of water activity: new results and an intercomparison of techniques for measuring the viscosity of particles, *Atmos. Meas. Tech.*, 11, 4809–4822, doi:10.5194/amt-11-4809-2018, 2018.

- Claeys, M.: Formation of secondary organic aerosols through photooxidation of isoprene, *Science*, 303, 1173–1176, doi:10.1126/science.1092805, 2004.
- Cody, R. B., Laramée, J. A. and Durst, H. D.: Versatile new ion source for the analysis of materials in open air under ambient conditions, *Anal. Chem.*, 77, 2297–2302, doi:10.1021/ac050162j, 2005.
- 5 Compernelle, S., Ceulemans, K. and Müller, J.-F.: EVAPORATION: a new vapour pressure estimation method for organic molecules including non-additivity and intramolecular interactions, *Atmos. Chem. Phys.*, 11, 9431–9450, doi:10.5194/acp-11-9431-2011, 2011.
- Davies, J. F., Miles, R. E. H., Haddrell, A. E. and Reid, J. P.: Influence of organic films on the evaporation and condensation of water in aerosol, *Proc. Natl. Acad. Sci.*, 110, 8807–8812, doi:10.1073/pnas.1305277110, 2013.
- 10 Davies, J. F. and Wilson, K. R.: Nanoscale interfacial gradients formed by the reactive uptake of OH radicals onto viscous aerosol surfaces, *Chem. Sci.*, 6, 7020–7027, doi:10.1039/c5sc02326b, 2015.
- D'Ambro, E. L., Lee, B. H., Liu, J., Shilling, J. E., Gaston, C. J., Lopez-Hilfiker, F. D., Schobesberger, S., Zaveri, R. A., Mohr, C., Lutz, A., Zhang, Z., Gold, A., Surratt, J. D., Rivera-Rios, J. C., Keutsch, F.
- 15 N. and Thornton, J. A.: Molecular composition and volatility of isoprene-photochemical oxidation secondary organic aerosol under low-and high-NO<sub>x</sub> conditions, *Atmos. Chem. Phys.*, 17, 159–174, doi:10.5194/acp-17-159-2017, 2017.
- Dennis-Smith, B. J., Miles, R. E. H., and Reid, J.P.: Oxidative aging of mixed oleic acid/sodium chloride aerosol particles, *J. Geophys. Res.*, 117, D20204, <https://doi.org/10.1029/2012JD018163>,
- 20 2012.
- Drewnick, F., Diesch, J.-M., Faber, P. and Borrmann, S.: Aerosol mass spectrometry: particle–vaporizer interactions and their consequences for the measurements, *Atmos. Meas. Tech.*, 8, 3811–3830, doi:10.5194/amt-8-3811-2015, 2015.
- Ekström, S., Nozière, B., and Hansson, H.: The cloud condensation nuclei (CCN) properties of 2-methyltetrols and C<sub>3</sub>–C<sub>6</sub> polyols from osmolality and surface tension measurements. *Atmos. Chem. Phys.*, 9, 973–980. doi:10.5194/acp-9-973-2009, 2009.
- 25



- Enami, S., Hoffmann, M. R. and Colussi, A. J.: Extensive H-atom abstraction from benzoate by OH-radicals at the air–water interface, *Phys. Chem. Chem. Phys.*, 18, 31505–31512, doi:10.1039/c6cp06652f, 2016.
- Estillore, A. D., Trueblood, J. V. and Grassian, V. H.: Atmospheric chemistry of bioaerosols: heterogeneous and multiphase reactions with atmospheric oxidants and other trace gases, *Chem. Sci.*, 7, 6604–6616, doi:10.1039/c6sc02353c, 2016.
- Fan, H., Masaya, T. W., and Goulay, F.: Effect of surface–bulk partitioning on the heterogeneous oxidation of aqueous saccharide aerosols, *Phys. Chem. Chem. Phys.*, 21, 2992–3001. doi:10.1039/c8cp06785f, 2019.
- George, I. J. and Abbatt, J. P. D.: Heterogeneous oxidation of atmospheric aerosol particles by gas-phase radicals, *Nat. Chem.*, 2, 713–722, doi:10.1038/nchem.806, 2010.
- Grayson, J. W., Evoy, E., Song, M., Chu, Y., Maclean, A., Nguyen, A., Upshur, M. A., Ebrahimi, M., Chan, C. K., Geiger, F. M., Thomson, R. J. and Bertram, A. K.: The effect of hydroxyl functional groups and molar mass on the viscosity of non-crystalline organic and organic–water particles, *Atmos. Chem. Phys.*, 17, 8509–8524, doi:10.5194/acp-17-8509-2017, 2017.
- Hajslova, J., Cajka, T., and Vaclavik, L.: Challenging applications offered by direct analysis in real time (DART) in food-quality and safety analysis, *TrAC-Trend Anal. Chem.*, 30, 204–218, <https://doi.org/10.1016/j.trac.2010.11.001>, 2011.
- He, Q.-F., Ding, X., Fu, X.-X., Zhang, Y.-Q., Wang, J.-Q., Liu, Y.-X., Tang, M.-J., Wang, X.-M. and Rudich, Y.: Secondary organic aerosol formation from isoprene epoxides in the Pearl River Delta, South China: IEPOX- and HMML-Derived Tracers, *J. Geophys. Res.: Atmos.*, 123, 6999–7012, doi:10.1029/2017jd028242, 2018.
- Houle, F. A., Hinsberg, W. D. and Wilson, K. R.: Oxidation of a model alkane aerosol by OH radical: the emergent nature of reactive uptake, *Phys. Chem. Chem. Phys.*, 17, 4412–4423, doi:10.1039/c4cp05093b, 2015.

- Hu, W. W., Campuzano-Jost, P., Palm, B. B., Day, D. A., Ortega, A. M., Hayes, P. L., Krechmer, J. E., Chen, Q., Kuwata, M., Liu, Y. J., Sá, S. S. D., McKinney, K., Martin, S. T., Hu, M., Budisulistiorini, S. H., Riva, M., Surratt, J. D., Clair, J. M. S., Wertz, G. I.-V., Yee, L. D., Goldstein, A. H., Carbone, S., Brito, J., Artaxo, P., Gouw, J. A. D., Koss, A., Wisthaler, A., Mikoviny, T., Karl, T., Kaser, L., Jud, W., Hansel, A., Docherty, K. S., Alexander, M. L., Robinson, N. H., Coe, H., Allan, J. D., Canagaratna, M. R., Paulot, F. and Jimenez, J. L.: Characterization of a real-time tracer for isoprene epoxydiols-derived secondary organic aerosol (IEPOX-SOA) from Aerosol Mass Spectrometer measurements, *Atmos. Chem. Phys.*, 15, 11807–11833, doi:10.5194/acp-15-11807-2015, 2015.
- Hu, W., Palm, B. B., Day, D. A., Campuzano-Jost, P., Krechmer, J. E., Peng, Z., Sá, S. S. D., Martin, S. T., Alexander, M. L., Baumann, K., Hacker, L., Kiendler-Scharr, A., Koss, A. R., Gouw, J. A. D., Goldstein, A. H., Seco, R., Sjostedt, S. J., Park, J.-H., Guenther, A. B., Kim, S., Canonaco, F., Prévôt, A. S. H., Brune, W. H. and Jimenez, J. L.: Volatility and lifetime against OH heterogeneous reaction of ambient isoprene-epoxydiols-derived secondary organic aerosol (IEPOX-SOA), *Atmos. Chem. Phys.*, 16, 11563–11580, doi:10.5194/acp-16-11563-2016, 2016.
- Huang, Y., Barraza, K. M., Kenseth, C. M., Zhao, R., Wang, C., Beauchamp, J. L. and Seinfeld, J. H.: Probing the OH oxidation of pinonic acid at the air–water interface using Field-Induced Droplet Ionization Mass Spectrometry (FIDI-MS), *J. Phys. Chem. A.*, 122, 6445–6456, doi:10.1021/acs.jpca.8b05353, 2018.
- Kanakidou, M., Seinfeld, J. H., Pandis, S. N., Barnes, I., Dentener, F. J., Facchini, M. C., Dingenen, R. V., Ervens, B., Nenes, A., Nielsen, C. J., Swietlicki, E., Putaud, J. P., Balkanski, Y., Fuzzi, S., Horth, J., Moortgat, G. K., Winterhalter, R., Myhre, C. E. L., Tsigaridis, K., Vignati, E., Stephanou, E. G. and Wilson, J.: Organic aerosol and global climate modelling: a review, *Atmos. Chem. Phys.*, 5, 1053–1123, doi:10.5194/acp-5-1053-2005, 2005.
- Karadima, K. S., Mavrantzas, V. G., and Pandis, S. N.: Insights into the morphology of multicomponent organic and inorganic aerosols from molecular dynamics simulations, *Atmos. Chem. Phys.*, 19, 5571–5587, <https://doi.org/10.5194/acp-19-5571-2019>, 2019.

- Kessler, S. H., Smith, J. D., Che, D. L., Worsnop, D. R., Wilson, K. R. and Kroll, J. H.: Chemical sinks of organic aerosol: kinetics and products of the heterogeneous oxidation of erythritol and levoglucosan, *Environ. Sci. Technol.*, 44, 7005–7010, doi:10.1021/es101465m, 2010.
- Kleindienst, T. E., Lewandowski, M., Offenberg, J. H., Edney, E. O., Jaoui, M., Zheng, M., Ding, X. and Edgerton, E. S.: Contribution of primary and secondary sources to organic aerosol and PM<sub>2.5</sub> at SEARCH Network Sites, *J. Air Waste Manage. Assoc.*, 60, 1388–1399, doi:10.3155/1047-3289.60.11.1388, 2010.
- Kourtchev, I., Ruuskanen, T., Maenhaut, W., Kulmala, M. and Claeys, M.: Observation of 2-methyltetrols and related photo-oxidation products of isoprene in boreal forest aerosols from Hyytiälä, Finland, *Atmos. Chem. Phys.*, 5, 2761–2770, doi:10.5194/acp-5-2761-2005, 2005.
- Kroll, J. H., Smith, J. D., Che, D. L., Kessler, S. H., Worsnop, D. R. and Wilson, K. R.: Measurement of fragmentation and functionalization pathways in the heterogeneous oxidation of oxidized organic aerosol, *Phys. Chem. Chem. Phys.*, 11, 8005–8014, doi:10.1039/b905289e, 2009.
- Kroll, J. H., Lim, C. Y., Kessler, S. H. and Wilson, K. R.: Heterogeneous oxidation of atmospheric organic aerosol: kinetics of changes to the amount and oxidation state of particle-phase organic carbon, *J. Phys. Chem. A*, 119, 10767–10783, doi:10.1021/acs.jpca.5b06946, 2015.
- Kwong, K. C., Chim, M. M., Hoffmann, E. H., Tilgner, A., Herrmann, H., Davies, J. F., Wilson, K. R. and Chan, M. N.: Chemical transformation of methanesulfonic acid and sodium methanesulfonate through heterogeneous OH oxidation, *ACS Earth Space Chem.*, 2, 895–903, doi:10.1021/acsearthspacechem.8b00072, 2018a.
- Kwong, K. C., Chim, M. M., Davies, J. F., Wilson, K. R. and Chan, M. N.: Importance of sulfate radical anion formation and chemistry in heterogeneous OH oxidation of sodium methyl sulfate, the smallest organosulfate, *Atmos. Chem. Phys.*, 18, 2809–2820, doi:10.5194/acp-18-2809-2018, 2018b.
- Lam, H. K., Shum, S. M., Davies, J. F., Song, M., Zuend, A., and Chan, M. N.: Effects of inorganic salts on the heterogeneous OH oxidation of organic compounds: insights from methylglutaric acid–

- ammonium sulfate, *Atmos. Chem. Phys.*, 19, 9581–9593, <https://doi.org/10.5194/acp-19-9581-2019>, 2019a.
- Lam, H. K., Kwong, K. C., Poon, H. Y., Davies, J. F., Zhang, Z., Gold, A., Surratt, J. D. and Chan, M. N.: Heterogeneous OH oxidation of isoprene-epoxydiol-derived organosulfates: kinetics, chemistry and formation of inorganic sulfate, *Atmos. Chem. Phys.*, 19, 2433–2440, doi:10.5194/acp-19-2433-2019, 2019b.
- Leaitch, W. R., Bottenheim, J. W., Biesenthal, T. A., Li, S.-M., Liu, P. S. K., Asalian, K., Dryfhout-Clark, H., Hopper, F. and Brechtel, F.: A case study of gas-to-particle conversion in an eastern Canadian forest, *J. Geophys. Res.: Atmos.*, 104, 8095–8111, doi:10.1029/1998jd100012, 1999.
- 10 Lewandowski, M., Jaoui, M., Kleindienst, T. E., Offenberg, J. H. and Edney, E. O.: Composition of PM<sub>2.5</sub> during the summer of 2003 in Research Triangle Park, North Carolina, *Atmos. Environ.*, 41, 4073–4083, doi:10.1016/j.atmosenv.2007.01.012, 2007.
- Li, W.; Pak, C. Y.; Wang, X.; Tse, Y.-L. S.: Uptake of common atmospheric gases by organic-coated water droplets, *J. Phys. Chem. C*, 123, 18924–18931, 2019.
- 15 Mao, J., Ren, X., Brune, W. H., Olson, J. R., Crawford, J. H., Fried, A., Huey, L. G., Cohen, R. C., Heikes, B., Singh, H. B., Blake, D. R., Sachse, G. W., Diskin, G. S., Hall, S. R. and Shetter, R. E.: Airborne measurement of OH reactivity during INTEX-B, *Atmos. Chem. Phys.*, 9, 163–173, doi:10.5194/acp-9-163-2009, 2009.
- McNeill, V. F., Wolfe, G. M., and Thornton, J. A.: The oxidation of oleate in submicron aqueous salt aerosols: Evidence of a surface process, *J. Phys. Chem. A*, 111, 1073–1083, 2007.
- 20 McNeill, V. F., Yatavelli, R. L. N., Thornton, J. A., Stipe, C. B., and Landgrebe, O.: Heterogeneous OH oxidation of palmitic acid in single component and internally mixed aerosol particles: vaporization and the role of particle phase, *Atmos. Chem. Phys.*, 8, 5465–5476, <https://doi.org/10.5194/acp-8-5465-2008>, 2008.
- 25 Marsh, A., Miles, R. E. H., Rovelli, G., Cowling, A. G., Nandy, L., Dutcher, C. S. and Reid, J. P.: Influence of organic compound functionality on aerosol hygroscopicity: dicarboxylic acids, alkyl-

substituents, sugars and amino acids, *Atmos. Chem. Phys.*, 17, 5583–5599, doi:10.5194/acp-17-5583-2017, 2017.

Marshall, F. H., Miles, R. E. H., Song, Y.-C., Ohm, P. B., Power, R. M., Reid, J. P. and Dutcher, C. S.: Diffusion and reactivity in ultra-viscous aerosol and the correlation with particle viscosity, *Chem. Sci.*, 7, 1298–1308, doi:10.1039/c5sc03223g, 2016.

Marshall, F. H., Berkemeier, T., Shiraiwa, M., Nandy, L., Ohm, P. B., Dutcher, C. S. and Reid, J. P.: Influence of particle viscosity on mass transfer and heterogeneous ozonolysis kinetics in aqueous-sucrose-maleic acid aerosol, *Phys. Chem. Chem. Phys.*, 20, 15560–15573, doi:10.1039/c8cp01666f, 2018.

10 Marcus, Y.: Ionic radii in aqueous solutions, *Chem. Rev.*, 88, 1475–1498, doi:10.1021/cr00090a003, 1988.

Masterton, W. L., Bolocofsky, D. and Lee, T. P.: Ionic radii from scaled particle theory of the salt effect, *J. Phys. Chem.*, 75, 2809–2815, doi:10.1021/j100687a017, 1971.

15 McNeill, V. F., Wolfe, G. M. and Thornton, J. A.: The Oxidation of oleate in submicron aqueous salt aerosols: evidence of a surface process, *J. Phys. Chem. A*, 111, 1073–1083, doi:10.1021/jp066233f, 2007.

McNeill, V. F., Yatavelli, R. L. N., Thornton, J. A., Stipe, C. B. and Landgrebe, O.: Heterogeneous OH oxidation of palmitic acid in single component and internally mixed aerosol particles: vaporization and the role of particle phase, *Atmos. Chem. Phys.*, 8, 5465–5476, doi:10.5194/acp-8-5465-2008, 2008.

20 Mukundan, T. and Kishore, K.: Synthesis, characterization and reactivity of polymeric peroxides, *Prog. Poly. Sci.*, 15, 475–505, doi:10.1016/0079-6700(90)90004-k, 1990.

Nah, T., Chan, M., Leone, S. R. and Wilson, K. R.: Real time in situ chemical characterization of submicrometer organic particles using direct analysis in Real Time-Mass Spectrometry, *Anal. Chem.*, 85, 2087–2095, doi:10.1021/ac302560c, 2013.

25 Olson, N. E., Lei, Z., Craig, R. L., Zhang, Y., Chen, Y., Lambe, A. T., Zhang, Z., Gold, A., Surratt, J. D. and Ault, A. P.: Reactive Uptake of Isoprene Epoxydiols Increases the Viscosity of the Core of

Phase-Separated Aerosol Particles, ACS Earth Space Chem., 3, 1402–1414, doi:10.1021/acsearthspacechem.9b00138, 2019.

Peeters, J., Fantechi, G. and Vereecken, L.: A generalized structure-activity relationship for the decomposition of (substituted) alkoxy radicals, J. Atmos. Chem., 48, 59–80, doi:10.1023/b:joch.0000034510.07694.ce, 2004.

Renbaum, L. H. and Smith G. D.: The importance of phase in the radical-initiated oxidation of model organic aerosols: reactions of solid and liquid brassidic acid particles, Phys. Chem. Chem. Phys., 11, 2441–2451, https://doi.org/10.1039/b816799k, 2009.

Riva, M., Chen, Y., Zhang, Y., Lei, Z., Olson, N. E., Boyer, H. C., Narayan, S., Yee, L. D., Green, H. S., Cui, T., Zhang, Z., Baumann, K., Fort, M., Edgerton, E., Budisulistiorini, S. H., Rose, C. A., Ribeiro, I. O., Oliveira, R. L. E., Santos, E. O. D., Machado, C. M. D., Szopa, S., Zhao, Y., Alves, E. G., Sá, S. S. D., Hu, W., Knipping, E. M., Shaw, S. L., Junior, S. D., Souza, R. A. F. D., Palm, B. B., Jimenez, J.-L., Glasius, M., Goldstein, A. H., Pye, H. O. T., Gold, A., Turpin, B. J., Vizuete, W., Martin, S. T., Thornton, J. A., Dutcher, C. S., Ault, A. P. and Surratt, J. D.: Increasing Isoprene Epoxydiol-to-Inorganic Sulfate Aerosol Ratio Results in Extensive Conversion of Inorganic Sulfate to Organosulfur Forms: Implications for Aerosol Physicochemical Properties, Environ. Sci. Technol., 53, 8682–8694, doi:10.1021/acs.est.9b01019, 2019.

Robinson, C. B., Schill, G. P. and Tolbert, M. A.: Optical growth of highly viscous organic/sulfate particles, J. Atmos. Chem., 71, 145–156, doi:10.1007/s10874-014-9287-8, 2014.

Rudich, Y., Donahue, N. M. and Mentel, T. F.: Aging of organic aerosol: bridging the gap between laboratory and field studies, Annu. Rev. Phys. Chem., 58, 321–352, doi:10.1146/annurev.physchem.58.032806.104432, 2007.

Russell, G. A.: Deuterium-isotope effects in the autoxidation of aralkyl hydrocarbons. mechanism of the interaction of peroxy radicals<sup>1</sup>, J. Am. Chem. Soc., 79, 3871–3877, doi:10.1021/ja01571a068, 1957.

- Schauer, J. J., Fraser, M. P., Cass, G. R. and Simoneit, B. R. T.: Source reconciliation of atmospheric gas-phase and particle-phase pollutants during a severe photochemical smog episode, *Environ. Sci. Technol.*, 36, 3806–3814, doi:10.1021/es011458j, 2002.
- Slade, J. H. and Knopf, D. A.: Multiphase OH oxidation kinetics of organic aerosol: The role of particle phase state and relative humidity, *Geophys. Res. Lett.*, 41, 5297–5306, doi:10.1002/2014gl060582, 2014.
- Shrivastava, M., Cappa, C. D., Fan, J., Goldstein, A. H., Guenther, A. B., Jimenez, J. L., Kuang, C., Laskin, A., Martin, S. T., Ng, N. L., Petaja, T., Pierce, J. R., Rasch, P. J., Roldin, P., Seinfeld, J. H., Shilling, J., Smith, J. N., Thornton, J. A., Volkamer, R., Wang, J., Worsnop, D. R., Zaveri, R. A., Zelenyuk, A. and Zhang, Q.: Recent advances in understanding secondary organic aerosol: Implications for global climate forcing, *Rev. Geophys.*, 55, 509–559, doi:10.1002/2016rg000540, 2017.
- Smith, J. D., Kroll, J. H., Cappa, C. D., Che, D. L., Liu, C. L., Ahmed, M., Leone, S. R., Worsnop, D. R. and Wilson, K. R.: The heterogeneous reaction of hydroxyl radicals with sub-micron squalane particles: a model system for understanding the oxidative aging of ambient aerosols, *Atmos. Chem. Phys.*, 9, 3209–3222, doi:10.5194/acp-9-3209-2009, 2009.
- Song, M., Marcolli, C., Krieger, U. K., Zuend, A. and Peter, T.: Liquid-liquid phase separation in aerosol particles: Dependence on O:C, organic functionalities, and compositional complexity, *Geophys. Res. Lett.*, 39, doi:10.1029/2012gl052807, 2012.
- Song, M., Marcolli, C., Krieger, U. K., Lienhard, D. M. and Peter, T.: Morphologies of mixed organic/inorganic/aqueous aerosol droplets, *Faraday Discuss.*, 165, 289, doi:10.1039/c3fd00049d, 2013.
- Song, Y. C., Haddrell, A. E., Bzdek, B. R., Reid, J. P., Bannan, T., Topping, D. O., Percival, C. and Cai, C.: Measurements and predictions of binary component aerosol particle viscosity, *J. Phys. Chem. A*, 120, 8123–8137, doi:10.1021/acs.jpca.6b07835, 2016.

- Socorro, J., Lakey, P. S. J., Han, L., Berkemeier, T., Lammel, G., Zetzsch, C., Pöschl, U.\* and Shiraiwa, M.: Heterogeneous OH oxidation, shielding effects and implications for the atmospheric fate of terbuthylazine and other pesticides, *Environ. Sci. Technol.*, 51, 13749-13754, 2017.
- Stark, H., Yatavelli, R. L. N., Thompson, S. L., Kang, H., Krechmer, J. E., Kimmel, J. R., Palm, B. B.,  
5 Hu, W. W., Hayes, P. L., Day, D. A., Campuzano-Jost, P., Canagaratna, M. R., Jayne, J. T., Worsnop,  
D. R., and Jimenez, J. L.: Impact of Thermal Decomposition on Thermal Desorption Instruments:  
Advantage of Thermogram Analysis for Quantifying Volatility Distributions of Organic Species,  
Environ. Sci. Technol., 51, 8491–8500, 2017.
- 10 Surratt, J. D., Murphy, S. M., Kroll, J. H., Ng, N. L., Hildebrandt, L., Sorooshian, A., Szmigielski, R.,  
Vermeylen, R., Maenhaut, W., Claeys, M., Flagan, R. C. and Seinfeld, J. H.: Chemical composition of  
secondary organic aerosol formed from the photooxidation of isoprene, *J. Phys. Chem. A*, 110, 9665–  
9690, doi:10.1021/jp061734m, 2006.
- Wennberg, P. O., Bates, K. H., Crounse, J. D., Dodson, L. G., Mcvay, R. C., Mertens, L. A., Nguyen,  
T. B., Praske, E., Schwantes, R. H., Smarte, M. D., Clair, J. M. S., Teng, A. P., Zhang, X. and Seinfeld,  
15 J. H.: Gas-phase reactions of isoprene and its major oxidation products, *Chem. Rev.*, 118, 3337–3390,  
doi:10.1021/acs.chemrev.7b00439, 2018.
- Xia, X. and Hopke, P. K.: Seasonal variation of 2-methyltetrols in ambient air samples, *Environ. Sci.*  
*Technol.*, 40, 6934–6937, doi:10.1021/es060988i, 2006.
- Xu, L., Guo, H., Boyd, C. M., Klein, M., Bougiatioti, A., Cerully, K. M., Hite, J. R., Isaacman-  
20 Vanwertz, G., Kreisberg, N. M., Knote, C., Olson, K., Koss, A., Goldstein, A. H., Hering, S. V., Gouw,  
J. D., Baumann, K., Lee, S.-H., Nenes, A., Weber, R. J. and Ng, N. L.: Effects of anthropogenic  
emissions on aerosol formation from isoprene and monoterpenes in the southeastern United States,  
*Proc. Natl. Acad. Sci.*, 112, 37–42, doi:10.1073/pnas.1417609112, 2014.
- You, Y., Renbaum-Wolff, L. and Bertram, A. K.: Liquid–liquid phase separation in particles containing  
25 organics mixed with ammonium sulfate, ammonium bisulfate, ammonium nitrate or sodium chloride,  
*Atmos. Chem. Phys.*, 13, 11723–11734, doi:10.5194/acp-13-11723-2013, 2013.



- You, Y., Smith, M. L., Song, M., Martin, S. T. and Bertram, A. K.: Liquid–liquid phase separation in atmospherically relevant particles consisting of organic species and inorganic salts, *Int. Rev. Phys. Chem.*, 33, 43–77, doi:10.1080/0144235x.2014.890786, 2014.
- Vereecken, L. and Peeters, J.: Decomposition of substituted alkoxy radicals—part I: a generalized structure–activity relationship for reaction barrier heights, *Phys. Chem. Chem. Phys.*, 11, 9062, doi:10.1039/b909712k, 2009.
- Veghte, D. P., Bittner, D. R. and Freedman, M. A.: Cryo-transmission electron microscopy imaging of the morphology of submicrometer aerosol containing organic acids and ammonium sulfate, *Anal. Chem.*, 86, 2436–2442, doi:10.1021/ac403279f, 2014.
- 10 Viecei, J.; Roeselova, M.; Potter, N.; Dang, L. X.; Garrett, B. C.; Tobias, D. J.: Molecular dynamics simulations of atmospheric oxidants at the air-water interface: solvation and accommodation of OH and O<sub>3</sub>, *J. Phys. Chem. B*, 109, 15876–15892, 2005.
- Zhang, C., and Carloni, P.: Salt effects on water/hydrophobic liquid interfaces: A molecular dynamics study, *J. Phys.: Condens. Matter*, 24(12), 124109. doi:10.1088/0953-8984/24/12/124109. 2012.
- 15 Zhang, H., Worton, D. R., Lewandowski, M., Ortega, J., Rubitschun, C. L., Park, J.-H., Kristensen, K., Campuzano-Jost, P., Day, D. A., Jimenez, J. L., Jaoui, M., Offenberg, J. H., Kleindienst, T. E., Gilman, J., Kuster, W. C., Gouw, J. D., Park, C., Schade, G. W., Frossard, A. A., Russell, L., Kaser, L., Jud, W., Hansel, A., Cappellin, L., Karl, T., Glasius, M., Guenther, A., Goldstein, A. H., Seinfeld, J. H., Gold, A., Kamens, R. M. and Surratt, J. D.: Organosulfates as tracers for secondary organic aerosol (SOA) formation from 2-methyl-3-buten-2-ol (MBO) in the atmosphere, *Environ. Sci. Technol.*, 46(17), 9437–9446, doi:10.1021/es301648z, 2012.
- 20 Zhang, Z.-S., Engling, G., Chan, C.-Y., Yang, Y.-H., Lin, M., Shi, S., He, J., Li, Y.-D. and Wang, X.-M.: Determination of isoprene-derived secondary organic aerosol tracers (2-methyltetrols) by HPAEC-PAD: Results from size-resolved aerosols in a tropical rainforest, *Atmos. Environ.*, 70, 468–476, doi:10.1016/j.atmosenv.2013.01.020, 2013.
- 25

Zhang, H., Worton, D. R., Shen, S., Nah, T., Isaacman-Vanwertz, G., Wilson, K. R. and Goldstein, A. H.: Fundamental time scales governing organic aerosol multiphase partitioning and oxidative aging, *Environ. Sci. Technol.*, 49, 9768–9777, doi:10.1021/acs.est.5b02115, 2015.

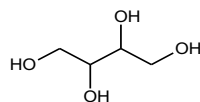
Zhang, Y., Chen, Y., Lei, Z., Olson, N. E., Riva, M., Koss, A. R., Zhang, Z., Gold, A., Jayne, J. T., Worsnop, D. R., Onasch, T. B., Kroll, J. H., Turpin, B. J., Ault, A. P. and Surratt, J. D.: Joint Impacts of Acidity and Viscosity on the Formation of Secondary Organic Aerosol from Isoprene Epoxydiols (IEPOX) in Phase Separated Particles, *ACS Earth Space Chem.*, 3, 2646–2658, doi:10.1021/acsearthspacechem.9b00209, 2019.

Zhao, Z., Xu, Q., Yang, X. and Zhang, H.: Heterogeneous ozonolysis of endocyclic unsaturated organic aerosol proxies: implications for criegee intermediate dynamics and later-generation reactions, *ACS Earth Space Chem.*, 3, 344–356, doi:10.1021/acsearthspacechem.8b00177, 2019.

Zuend, A., Marcolli, C., Luo, B. P., and Peter, T.: A thermodynamic model of mixed organic-inorganic aerosols to predict activity coefficients, *Atmos. Chem. Phys.*, 8, 4559-4593, <https://doi.org/10.5194/acp-8-4559-2008>, 2008.

Zuend, A., Marcolli, C., Booth, A. M., Lienhard, D. M., Soonsin, V., Krieger, U. K., Topping, D. O., Mcfiggans, G., Peter, T. and Seinfeld, J. H.: New and extended parameterization of the thermodynamic model AIOMFAC: calculation of activity coefficients for organic-inorganic mixtures containing carboxyl, hydroxyl, carbonyl, ether, ester, alkenyl, alkyl, and aromatic functional groups, *Atmos. Chem. Phys.*, 11, 9155–9206, doi:10.5194/acp-11-9155-2011, 2011.

**Table 1.** Chemical structure, properties, effective rate constant and OH uptake coefficient of pure erythritol particles and erythritol–AS particles with different IORs at 85 % RH.

Compounds		Erythritol			
Structural Formula					
Molecular Formula		C <sub>4</sub> H <sub>10</sub> O <sub>4</sub>			
Molecular Weight (g mol <sup>-1</sup> )		122.12			
Particle Composition					
Inorganic-to-Organic Mass Ratio (IOR)	0.0 (Pure)	0.5	1.0	5.0	
Sulfate-to-Organic Mass Ratio	0.0 (Pure)	0.36	0.72	3.64	
Mass Fraction of Erythritol (%)	47.3	28.0	19.9	6.1	
Mass Fraction of AS (%)	0.0	14.0	19.9	30.5	
Mass Fraction of Water (%) <sup>a</sup>	52.7	58.0	60.2	63.4	
<u>Initial Mean Surface-Weighted</u>	<u>276.1</u>	<u>278.2</u>	<u>280.5</u>	<u>281.2</u>	
<u>Particle Diameter (GSD) (nm)</u>	<u>(~1.2)</u>	<u>(~1.3)</u>	<u>(~1.3)</u>	<u>(~1.3)</u>	
Particle Density (g cm <sup>-3</sup> )	1.172 ± 0.010	1.175 ± 0.005	1.177 ± 0.004	1.182 ± 0.001	
Effective Saturation Vapor Pressure of Erythritol, C* (μg m <sup>-3</sup> ) <sup>b</sup>	0.686	0.792	0.921	1.60	
Effective Heterogeneous OH					
Oxidation Rate Constant, <i>k</i> (×10 <sup>-13</sup> cm <sup>3</sup> molecule <sup>-1</sup> s <sup>-1</sup> )	5.38 ± 0.12	4.00 ± 0.04	3.26 ± 0.05	1.56 ± 0.04	
Effective OH Uptake Coefficient, $\gamma_{\text{eff}}$	0.45 ± 0.025	0.20 ± 0.010	0.12 ± 0.006	0.02 ± 0.001	
Chemical lifetime (days) <sup>c</sup>	14.3 ± 0.33	19.3 ± 0.22	23.6 ± 0.37	49.5 ± 1.43	

<sup>a</sup> The amount of water is predicted using the aerosol thermodynamic model at 85 % RH before oxidation

5 <sup>b</sup> Effective saturated vapor pressure of erythritol predicted before oxidation

<sup>c</sup> 24-h averaged OH concentration of  $1.5 \times 10^6$  molecules cm<sup>-3</sup>

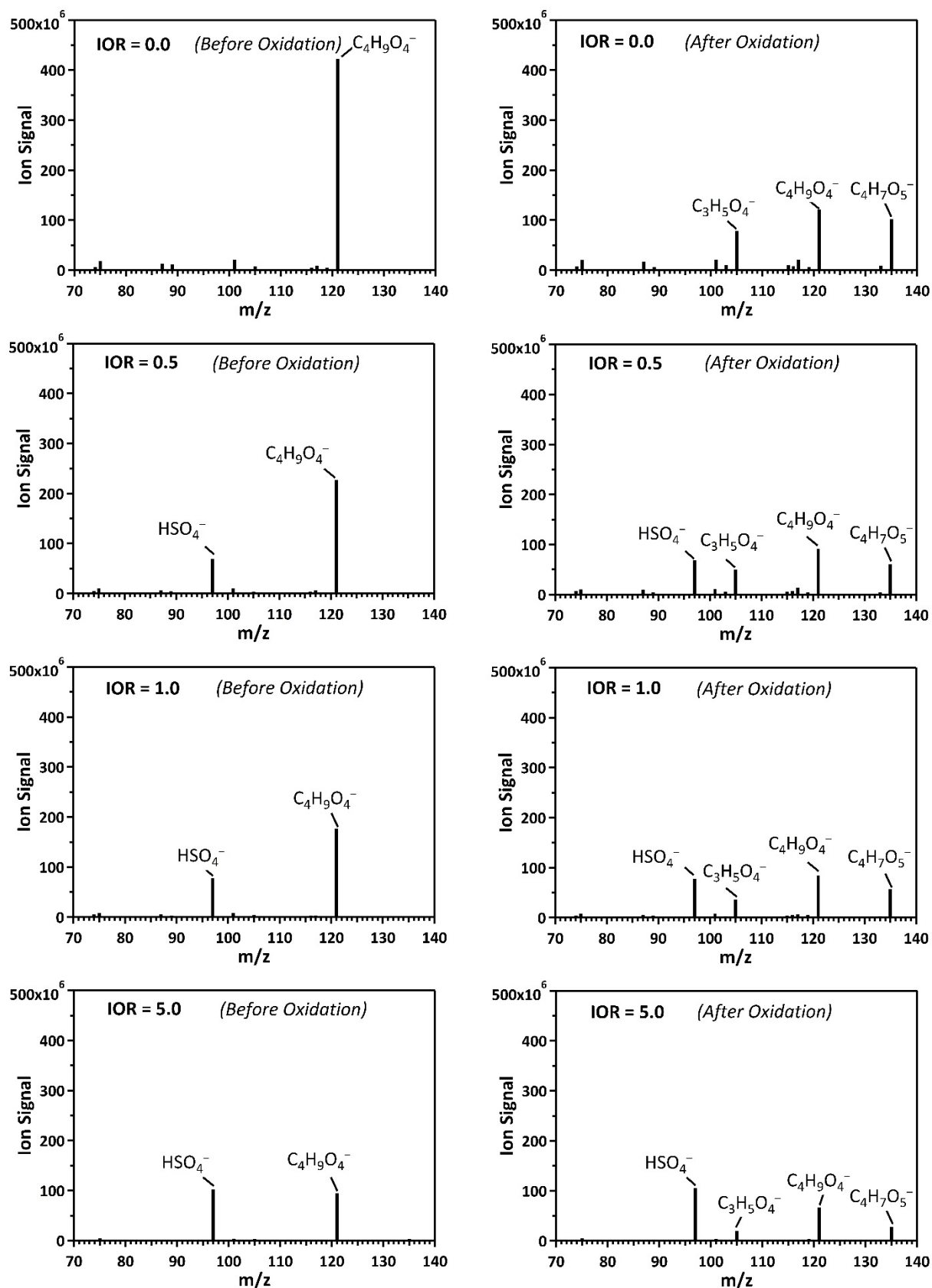


**Figure 1.** Particle-DART mass spectra for erythritol particles and erythritol-AS particles at different IORs before and after oxidation (at the highest OH exposure of  $\sim 2.29 \times 10^{12}$  molecule  $\text{cm}^{-3}$  s).

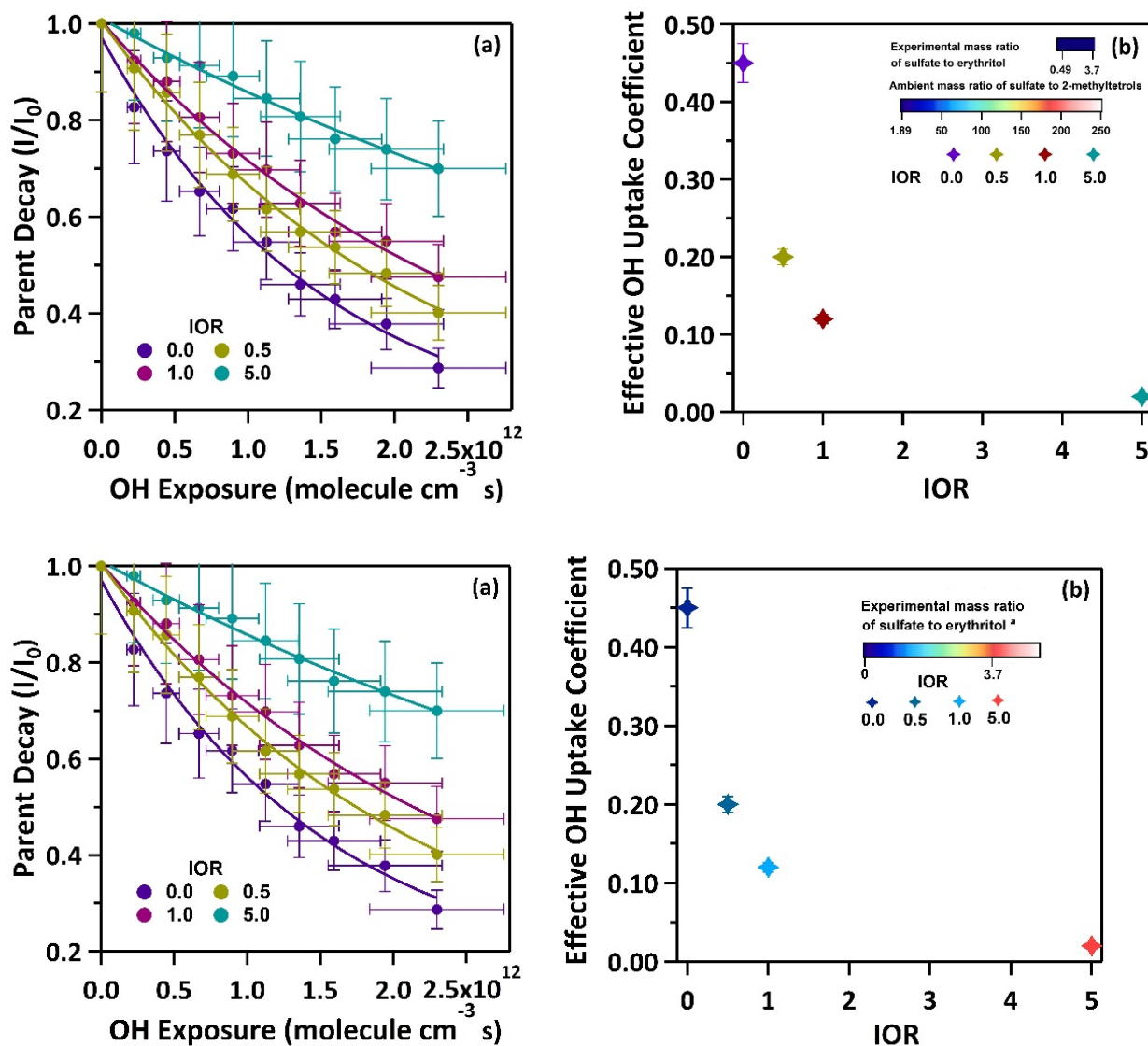


**Figure 2.** (a) The normalized decay of erythritol as a function of OH exposure during the heterogeneous OH oxidation of erythritol particles and erythritol-AS particles with different IORs. (b)

5 The effective OH uptake coefficient,  $\gamma_{\text{eff}}$ . The data points represent  $\gamma_{\text{eff}}$  value at different IORs. The color scales represent the range of corresponding sulfate to erythritol mass ratio (0 – 3.7) at different IORs in this work, much smaller than that for ambient mass ratio of sulfate to 2-methyltetrols reported in field studies ( $\sim 1.89 - \sim 250$ ). **Figure 2.** (a) The normalized decay of erythritol as a function of OH exposure during the heterogeneous OH oxidation of erythritol particles and erythritol-AS particles with different IORs. (b) The effective OH uptake coefficient,  $\gamma_{\text{eff}}$ .

10

